LA-UR- 08-7070

Approved for public release; distribution is unlimited.

Title:	The impact of CO2 on shallow groundwater chemistry: observations at a natural analog site and implications for carbon sequestration
Author(s):	Elizabeth Keating, Julianna Fessenden, Nancy Kanjorski, Dan Koning, and Rajesh Pawar
Intended for:	Environmental Geology

Los Alamos
NATIONAL LABORATORY
EST. 1943

Form 836 (7/06)

The impact of CO_2 on shallow groundwater chemistry: observations at a natural analog site and implications for carbon sequestration

Elizabeth Keating[1], Julianna Fessenden[1], Nancy Kanjorski[2], Dan Koning[3], and Rajesh Pawar[1]

[1]Earth and Environmental Sciences Division, Los Alamos National Laboratory
[3]New Mexico Bureau of Geology and Mineral Resources

Abstract

In a natural analog study of risks associated with carbon sequestration, impacts of CO_2 on shallow groundwater quality have been measured in a sandstone aquifer in New Mexico, USA. Despite relatively high levels of dissolved CO_2, originating from depth and producing geysering at one well, pH depression and consequent trace element mobility are relatively minor effects due to the buffering capacity of the aquifer. However, local contamination due to influx of saline waters in a subset of wells is significant. Geochemical modeling of major ion concentrations suggests that high alkalinity and carbonate mineral dissolution buffers pH changes due to CO_2 influx. Analysis of trends in dissolved trace elements, chloride, and CO_2 reveal no evidence of in-situ trace element mobilization. There is clear evidence, however, that As, U, and Pb are locally co-transported into the aquifer with CO_2-rich saline water. This study illustrates the role that local geochemical conditions will play in determining the effectiveness of monitoring strategies for CO_2 leakage. For example, if buffering is significant, pH monitoring may not effectively detect CO_2 leakage. This study also highlights potential complications that CO_2 carrier fluids, such as saline waters, pose in monitoring impacts of geologic sequestration.

Introduction

There is understandable concern about possible impacts to shallow aquifers if CO_2 were to leak from primary storage reservoirs during or after geologic sequestration operations. There is a paucity of field data, however, to characterize the nature of potential impacts. Undesirable side affects might include catastrophic release of CO_2 at the surface (e.g. well blow-out) and leakage of brine (Benson, 2002; Kharaka et al., 2006). Although CO_2 is not toxic in low concentrations, dissolution into shallow groundwater may depress pH and subsequent trace metal dissolution from aquifer minerals may increase the concentration of naturally-occurring toxic elements such as lead and arsenic (Benson, 2002; Wang and Jaffe, 2004). Predicting the potential impact of CO_2 release in shallow aquifers at any sequestration site is a challenging task. There are at least three possible research strategies for evaluating this type of effect, all of which have strengths and limitations. One is to directly monitor shallow aquifer chemistry at engineered CO_2 sequestration sites where CO_2 is leaking upward at a known rate. This may not be feasible because engineered sites are generally thought NOT to be leaking, by design, and so directly measuring the impacts of leaks is difficult. Even if leaks do occur, few sites have background groundwater monitoring programs in place

that would allow quantitative comparison of pre- and post-leak water quality (Liewicki et al., 2007). Leaks may be difficult to detect due to limitations in infrastructure, low density of wells, and infrequent measurements. Consequently, establishing robust monitoring strategies and characterizing background geochemical conditions has become a high priority at some engineered sites (Smyth et al., 2006). Another strategy involves using mineralogy and water quality data collected from a variety of aquifer types that might ultimately receive CO_2 leaks and *predict* possible impacts using geochemical theory (Birkholzer et al., 2007; Birkholzer 2008) This strategy can provide insight into processes that may ultimately be important. However, the predictive ability of studies like these will always be limited by irreducible uncertainty in field-scale mineral dissolution kinetic rates and local-scale heterogeneity in aquifer mineralogy. Mechanistic-based approaches to measuring kinetics are only possible in the laboratory under well-controlled conditions (Bose and Sharma, 2002; Bruno et al., 1992; Craw et al., 2003; Golubev et al., 2005; Stephens and Hering, 2004). Unfortunately, large discrepancies between field and laboratory rate estimates (Chen, 2005; Langmuir, 1997) contributes to uncertainty in predictive modeling. The impact of uncertainty in kinetic rate on predicting trace metal mobility due to CO_2 leaks has been well documented (Wang and Jaffe, 2004). Another factor which will limit the predictive ability of geochemical models is the difficulty of predicting scavenging of trace metals by secondary minerals such as carbonates, iron oxy-hydroxides and clay minerals (Aiuppa et al., 2005). Without validation at natural or engineered analog sites where CO_2 is present at significant concentrations, it will be difficult to assess the accuracy of this modeling-based approach.

A third approach, utilized in this study, involves directly measuring CO_2 impacts at a natural analog site where CO_2 is actively upwelling through a shallow aquifer. These sites are usually located in volcanic or geothermal settings (Federico et al., 2004; Glennon, 2005; Lu et al., 2005). Like the other two strategies, this empirical approach has inherent limitations. Most importantly, the highly fractured geologic settings where active CO_2 upwelling occurs naturally are very unlikely to be considered for geologic sequestration (Benson, 2002). In addition, the lack of "pre CO_2 flux" water quality data inhibits comparison of pre- and post-CO_2 conditions. The aquifer may not be impacted only by CO_2, but rather a mixture of CO_2 and deep thermal waters of unknown origin and/or composition. A dense network of wells available for shallow groundwater characterization may not be available. With these caveats in mind, we present field observations and interpretations of a site in Northern New Mexico with active CO_2 upwelling through a shallow aquifer. A number of domestic wells are available for sampling, offering an opportunity to compare background groundwater quality and CO_2-impacted groundwater quality. Conclusions follow, with implications for CO_2 sequestration leakage scenarios and monitoring strategies.

Natural analog sites for studying CO_2 impacts on aquifers

There are two major categories of natural analogs: 1) locations where diffuse CO_2 is rising and flowing through an aquifer (where it can be measured in wells), and 2) locations where CO_2 is rising along a fault or other conduit and expresses itself at a point at the ground surface (a spring or a geyser) (**Figure 1**). Studies of the second type are

far more common, due in part to the ease of sampling springs or geysers. Studies of CO_2-charged springs (Glennon, 2005; Goff et al., 1988; Newell et al., 2005; Vuataz et al., 1984) provide insight into the dynamics of CO_2 flow and into geochemical processes occurring at depth, but they are not particularly informative about the impact of CO_2 on *aquifers*, since the CO_2 may not significantly impact a shallow aquifer if it rises along a conduit and rapidly discharges at a spring (**Figure 1a**). However, the extent that CO_2 upwelling along faults mixes with local groundwater may be assessed by temperature and trace elements
(Vautaz et al., 1984).

Far less common are studies of *aquifer* chemistry in CO_2 rich settings that include samples from both wells and springs. Very comprehensive studies on groundwater chemistry in high CO_2 flux settings have been performed on volcanoes in Italy (Aiuppa et al., 2005; Federico et al., 2004). Here, large datasets on groundwater chemistry in aquifers (including but not limited to springs) have been collected and analyzed using very sophisticated geochemical modeling. The authors were able to discriminate between trace metal concentrations controlled by availability in aquifer materials (As, Cd, Mo, Se, V) and trace metal concentrations controlled by kinetically-controlled mineral dissolution/precipitation. Because of dissolution / desorption of trace metals from aquifer minerals and subsequent scavenging by secondary minerals (primarily calcite), no trends in trace element concentrations with pCO_2 or pH (range 5.8 – 8.0) were measured. Mammoth Mountain, CA (Rogie et al., 2001) also represents a diffuse CO_2 flux volcanic setting. Here, CO_2 flux resulted in localized tree mortality. Elevated trace metal concentration and depressed pH (near 4.0) were measured in the soil profile; however, geochemical data measured in springs and wells did not show a clear relation between elevated trace metal concentrations in groundwater with either pH (5.1 – 8.46) or pCO_2. One conclusion drawn by the authors was that the effect of upwelling CO_2 is "substantially neutralized" by mineral weathering, which in turn increases the total dissolved solids (TDS) of the fluid (Evans et al., 2002).

The site described in this study not only has a CO_2 expression at the ground surface (e.g., eruptions of a cold geyser) but also in a number of nearby shallow wells that are used for domestic drinking water purposes (Cumming, 1997). The source of the deep upwelling CO_2 remains uncertain, but normal faulting associated with the Rio Grande rift likely facilitates upwelling of deep fluids from Paleozoic sedimentary rocks (Cumming, 1997). For this study, we focus on documenting and interpreting the measurable effects of CO_2 on shallow groundwater chemistry, with particular emphasis on trace elements (F, U, Pb, As, and Fe).

Hydrogeologic setting

The community of Chimayó, New Mexico lies near the eastern margin of the Espanola Basin. Formed by extension associated with the Rio Grande Rift, the Espanola Basin is semi-arid, with rainfall ranging from 8 in/yr in the lower elevations to approximately 25 in/yr in the high mountains. Upper Oliogcene to upper Miocene alluvial- fan sandstones, comprising the Tesuque Formation of Santa Fe Group, serves as the aquifer for many communities including Chimayó (**Figure 2**). These sediments are quartz and feldspar rich; approximately 50-70 % of the felspars are plagioclase (Cavazza,

1986). Locally, secondary calcite is abundant typically regional groundwaters are in equilibrium with this mineral (Keating and Warren, 1999). Rock/water reactions, including weathering of calcite and plagioclase and precipitation of smectite, have been shown to explain trends in major ion chemistry in the regional aquifer (Hereford et al., 2007; Keating and Warren, 1999). Cross-sections suggest the aquifer is fairly thin in the vicinity of Chimayó (200-400 m thick; **Figure 3**). A wildcat oil well (Castle Wigzell Kelley Federal No. 1), located 3.5 km to the southwest of Chimayo, encountered Pennsylvanian carbonate and siltstone beneath the Tesuque Formation. It is likely that Pennsylvanian strata extend northeast to Chimayo, but reverse faulting from Laramide tectonism may have facilitated local erosional stripping of Pennsylvanian strata under Chimayo; similar erosion from Laramide uplift has been interpreted 10 km to the west (Baldridge et al., 1994). Both the Santa Fe Group and underlying carbonates are dissected by numerous north-south trending faults created by tectonic extension, some of which are cemented with calcite and/or siliceous minerals. Geologic mapping to the south suggests Proterozoic crystalline rocks directly underlies the Pennsylvanian strata (Koning et al., 2002).

Cumming (1997) conducted sampling of wells in the Chimayó community and noticed a strong tendency for shallow wells (depth < 60m) located near a particular fault to be enriched in dissolved CO_2. This fault was subsequently mapped in detail by Koning et al., 2002). Cumming (1997) generated a relatively large geochemical dataset (18 wells, most of which were sampled 4 times over a 2-year period). For all but two of the wells, only major ion chemistry is available.

One well in the community geysers approximately twice a day, releasing 99.9% pure CO_2. Although the geyser discharge is cyclical, the rate of influx of CO_2 into the aquifer from depth may be relatively constant (Lu, 2005). Eruption frequency is a function of recharge rate (influx to the bottom of the pipe), and the ratio of length to diameter of the pipe. The fact that only this particular well acts as a geyser may be due to it penetrating a fault-sealed pocket of the aquifer that has locally resulted in high P_{CO2}. This east-down fault, called the Roberts fault, exhibits surface evidence of intensive silica cementation.

At this site, the source of the CO_2 recharging the aquifer from below is unclear. Based on limited measurements of carbon isotopes, Cumming (1997) suggested that although the data are inconclusive, the most likely source was mantle CO_2. Another possibility, although discounted by the author based on temperature and pressure conditions in the basin, is thermal decarbonation of carbonate rock layers below the Santa Fe Group aquifer A third possibility is dissolution of carbonate rocks by acidic groundwater (a non-CO_2 source of acidity). No such waters have been measured in the Espanola Basin; this possibility seems remote. Without more detailed data collection it is impossible to definitively identify the CO_2 source.

There are three mechanisms which could be producing tendency to rise: 1) CO_2 rising as discreet pockets of buoyant gas, 2) groundwater with high levels of dissolved CO_2 and/or bubbles, which is less dense than background water and thus rises, and/or 3) upward head groundwater. If the fault mapped by Koning (2005) provides a pathway for CO_2 to move upward from depth, it is unclear exactly how the CO_2 moves within the fault zone. In this paper, we do not address either the source of the CO_2 or the

mechanism for upward movement. Rather, we focus on the impact of the CO_2 on shallow groundwater chemistry.

To provide context for this study, published groundwater chemistry datasets from 200 wells in the Espanola Basin, east of the Rio Grande, were combined and plotted on a Durov diagram (**Figure 4**) (McQuillan, 1998; USGS 1997; New Mexico Environment Department, 1980, 2003; Street, 2004). These regional groundwaters are generally either Ca-HCO_3 or Na-HCO_3-type waters. Median values of pH, Cl, and total dissolved solids (TDS) are 8.0, 12.5 mg/l, and 467 mg/l, respectively. As is evident in **Figure 4**, compared to typical regional groundwaters, data collected by Cumming (1997) in the Chimayo community aquifer tends to be significantly lower in pH and, in some wells, *much* higher in total dissolved solids. Due to the semi-arid environment, thick basin-fill (up to 3-4 km; Cordell, 1979), and hetereogeneity resulting from faults and dipping strata of various permeabilites, groundwaters in the Espanola Basin may move relatively slowly and may be very old (in some cases, tens of thousands of years old (Anderholm, 1994; Rogers et al., 1996)) and frequently enriched in naturally-occurring trace elements including flouride, uranium, and arsenic (Finch, 2005; Gallaher et al., 2004; McQuillan and Montes, 1998; Purtymun, 1977). Warm springs (<54°C) are present approximately 25 km to the north of Chimayó. These Na-HCO_3 type waters, enriched in Li, B, and F, are thought to be upwelling from depth along faults (Vuataz et al., 1984). Cummings (1997) reported that temperatures in Chimayó groundwaters range from 7 – 24°C, and are either Ca-HCO_3 or Na-HCO_3 type waters. Interestingly, although these waters are significantly cooler than the warm springs to the north, they are significantly higher in TDS (over 6,000 mg/l (Cumming 1997) versus 3600 mg/l) and more enriched in Cl. Br/Cl ratios in the geyser waters are similar to seawater. All waters sampled by Cumming (1997) were oxidizing, consistent with measured dissolved oxygen ranging from 0.4 to 9.3 mg/l. This is typical for the regional aquifer, where due to low availability of organic carbon and thick unsaturated zones (> 300 m in some locations) oxygen availability is rarely exceeded by microbial demand. Exceptions to this include local reducing conditions related to domestic septic effluent (personal communication, McQuillan, 2003).

Geochemical sampling

Our goal was to expand the number of domestic drinking water wells originally sampled by Cumming (1997) and to analyze for major ions, trace elements, and stable isotopes (^{13}C, ^{18}O, ^{2}H). The number of wells available for sampling was limited, however, because many homeowners in the community have recently abandoned their wells and connected to a community water supply. In total, we sampled 17 wells (**Figure 2**), four of which were also sampled by Cumming (1997) including the geyser well (#17). The combined dataset represents 31 wells.

Slightly more than half of the samples were collected from hose bibs, the rest were collected at the kitchen tap. When possible, the water was allowed to flow for one minute before sampling. All the samples were untreated and came directly from the well. One sample (McCormick well) was taken from a storage tank where groundwater and surface water are mixed. Sample bottles were filled to the rim and capped within seconds of collection to minimize exposure to air. Samples were tested for pH within one

to two hours of collection using a Thermo Electron Corporation probe. Samples for cation analysis were passed through a 0.05 μm filter. Samples were analyzed for major anions using Ion Chromotography, for cations using ICP-MS, for alkalinity using acid titration, and for stable isotopes using a multiflow unit connected to an isotope ratio mass spectrometer.

Sampling results

The chemical data was analyzed using the geochemical modeling code (PHREEQC) (Parkhurst and Appelo, 1999) and partial pressure of CO_2 (P_{CO2}) was calculated for all the sampled wells based on measured pH and alkalinity. For reference, atmospheric $P_{CO2} = 10^{-3.5}$ atm. The results of these calculations and all other chemical analyses are presented in **Tables 1-3**. Sixteen of the seventeen samples have calculated pCO_2 ($\log(P_{CO2})$) greater than or equal to -2.5; fifteen samples were $pCO_2 > -2.0$. This leads us to believe CO_2 degassing during sampling did not significantly affect our pH measurements (and hence pCO_2 calculations). We re-measured pH at the well with the lowest calculated pCO_2 (-3.3) and confirmed the relatively high pH (8.5). This well is used below to represent background conditions, unaffected by CO_2 upwelling.

To examine spatial and temporal variation in major ions, we combined this dataset with data presented by Cummings (1997) to extend the number of samples included in the study. Combining these datasets, collected several years apart, does introduce the possibility that temporal trends will be misinterpreted as spatial trends. However, spatial trends in pCO_2 , TDS, and [Cl] (**Figure 5**) are generally consistent in the two datasets and so temporal variability is presumably smaller than spatial variability. Values of pCO_2 significantly larger than atmospheric (up to -2.0) may possibly be caused by biologic activity in the vadose zone during recharge; however, this increase would then typically be offset by mineral weathering reactions in the aquifer. Because organic matter content tends to be low in this setting, we presume waters with pCO_2 greater than -2 represents groundwater impacted to some degree by influx of CO_2 from depth (beneath the aquifer). There are two clusters of wells with very high pCO_2; one near the south end of the minor fault (Roberts fault). The other cluster occurs where this minor fault projects northwards under Quaternary alluvium to the Chimayo fault. Wells near the Roberts fault (within approximately 500 m of the fault trace) tend to have higher pCO_2, (as large as 0), than wells farther from the fault. Not all wells near the fault have high pCO_2, which may be due to complexities in the path of the upwelling CO_2 and/or mixing and buffering reactions. The wells near the fault trace (within ~500 m) have higher TDS (up to 7000 mg/l) (**Figure 5b**). On the other hand the concentration of chloride is much higher at the southern end of the fault than other locations (**Figure 5c**). The increased levels of chloride are important to note as there is no local source for chloride in the shallow aquifer . Evaporite layers are known to exist below the Santa Fe Group in some portions of the basin, but were not present in the nearest deep well (Kelly Federal well). Since there are no evaporate minerals within the Santa Fe Group, the spatial trends in pCO_2 and [Cl] in **Figure 5** suggest that CO_2 is upwelling with deeper saline waters near the southern end of the fault and is upwelling without deeper saline waters near the northern end of the fault. Two different relationships between chloride and pCO_2 are evident in the data, as shown in **Figure 6**. The lowest chloride and pCO_2 wells samples

(lower left corner of **Figure 6**) represent dilute background waters, presumably recharged from meteoric sources either in the Sangre de Cristos mountain to the east or locally along the Santa Cruz River. These have relatively high pH and low [Cl] typical of other waters in the basin. In most of the wells sampled, however, the waters have been impacted to some extent by either CO_2 from depth or a CO_2-saline water mixture from depth. Depending on the degree of mixing and mineral precipitation/dissolution reactions in the aquifer, background waters either evolve towards high pCO_2/ low chloride waters (**Path 1, Figure 6**) or high pCO_2/ high chloride waters (**Path 2, Figure 6**). These two cases have very different implication for trace element mobilization and transport, as will be described below.

The stable isotope measurements are shown in **Figures 7 and 8**. In contrast to a large number of groundwaters sampled in the region which plot relatively close to the world meteoric line (WML) (Anderholm, 1994), Chimayó waters have $\delta^{18}O$ / δD ratios slightly shifted to the right (**Figure 7**). This can either be interpreted to reflect evaporation or deep circulation (long residence times and/or high temperatures. Stable isotopes measured in cold, meteoric groundwaters in this basin generally show no evidence of evaporation (Anderholm, 1994; Blake et al., 1995) and it is difficult to imagine a scenario where Chimayó groundwaters have experienced significant evaporation. A more likely scenario involves mixing of meteoric waters with deeper waters that had very long residence times in host rocks, similar to path 2 in **Figure 6**. This explanation was suggested by Vautaz et al. (1986) for a subset of waters in the Jemez Mountains (to the west) with similar departures from the WML.

As shown in **Figure 8a**, waters with higher pCO_2 values tend to be relatively enriched in ^{13}C. We would expect dissolved carbon in meteorically-recharged background waters to be isotopically light (-12 to -15 per mil) and deeper sources of carbon (either mantle and/or marine-carbonate derived) to be isotopically heavy (-4 to +4 per mil). Therefore, qualitatively this trend is consistent with the deep water mixing model presented above. In addition to the deep waters being isotopically heavy, they may become further enriched in ^{13}C by degassing CO_2 as they upwell. Unless waters are fairly acidic ($pH < 5.4$), CO_2 gas exsolved from groundwater will be isotopically lighter than the remaining dissolved carbon, as observed in Mammoth Lake groundwaters (Evans et al., 2002) and in laboratory experiments (Mook, 1974). In the geyser well samples, Cummings reported a value of $\delta^{13}C = -7.11$ for CO_2 gas relative to -0.55 ‰ in dissolved carbon.

The relationship between chloride and $\delta^{13}C$, shown in **Figure 8b**, clearly indicates two populations of waters, as was evident in **Figure 6**. The CO_2-rich saline waters near the south end of the Roberts fault are more enriched in heavy $\delta^{13}C$ and much higher in chloride than all the other waters. This suggests the CO_2 upwelling beneath much of the aquifer is less depleted in ^{13}C than the CO_2 upwelling along with saline waters near the southern end of the fault. Two possible explanations are as follows. Compared to upwelling CO_2 in locations other than the south end of the Roberts fault, the upwelling CO_2-rich saline waters either originated at depth at higher pressures, and thus degassed more as they rose, or interacted with isotopically heavier marine carbonate rocks (or both). The possible relationship between higher pressures, more intense degassing, and higher salinity will be explored in future work.

Discussion of transport mechanisms and geochemical modeling

The spatial variability in levels of dissolved CO_2 in Chimayó groundwater (**Figure 5a**) could be caused by a number of factors: 1) spatial variability in the flux of CO_2 into the aquifer (regardless of its source) 2) heterogeneity within the aquifer which causes CO_2 to build up in some locations, perhaps because of fault-sealing, and to diffuse to the vadose zone quickly in other locations, or 3) spatially-variable CO_2 consuming reactions such as calcite or plagioclase weathering. In addition to spatial variation in CO_2, there is large variation in chloride concentrations. This variation is likely due to processes occurring below the aquifer, as CO_2 diffuses through older sediments. Understanding the role that mineral weathering plays within the aquifer is important to risk assessment studies because weathering will tend to buffer pH changes. This potentially reduces risk to human health since trace element mobility, caused by pH reduction, may be prevented. A negative consequence, however, is that detection of CO_2 leakage via monitoring groundwater pH will be more difficult.

To examine the role of mineral weathering plays within the aquifer, geochemical models were constructed using the geochemical modeling code PHREEQC and results were compared to measured trends in water chemistry. The water chemistry data were separated into the two groups described above (saline, [Cl]>100 mg/l, and non-saline, [Cl], 100 mg/l). First, the progressive reaction of CO_2 with background water (represented by Well 15 (Table 1)) was modeled, and results were compared to measured variation in pH, HCO_3, pCO_2 in the low [Cl] waters. Possible dissolution/precipitation of calcite, which is ubiquitous as a secondary mineral in these sediments, was also considered. Weathering of plagioclase and other silicates is also known to occur in this basin (Cavazza, 1986; Hereford et al., 2007; Keating and Warren, 1999), however, dissolution rates are known to be much slower than for carbonate minerals and thus their impact would be a second-order effect. This is supported by our calculated saturation indices for groundwaters in Chimayó, which show that these waters are generally near or at equilibrium with respect to calcite and strongly undersaturated with respect to commonly occurring silicate minerals. We considered two cases:

- Model A: stepwise reaction of background groundwater with increasing amounts of CO_2, while maintaining equilibrium with calcite
- Model B: stepwise reaction of background groundwater with increasing amounts of CO_2, with no mineral reactions

Results of these calculations are shown in **Figure 9**, in comparison to measured chemical compositions for all waters with low chloride concentrations (< 100 mg/l). The data show a tendency for [Ca] to increase and for pH to decrease with increasing pCO_2. Model A (no calcite dissolution) greatly underpredicts calcium concentrations and overpredicts pH depression. In contrast, Model B matches the data reasonably well, except for at the highest pCO_2 values where predicted [Ca] is too high. Sensitivity studies showed that this discrepancy may be due to neglecting other mineral weathering reactions, such as feldspar dissolution, which may become important at the highest pCO_2 values. Other than these highest pCO_2 calculations, departures of modeled trends from measured trends are unbiased and so are presumably caused by a combination of

measurement errors (particularly pH) and natural variability in background water composition, aquifer mineralogy, and mineral dissolution rates. It is noteworthy that a significant percentage of the measured variability in pH, pCO_2, and calcium of these low chloride waters can be described by two simple reactions: influx of CO_2 and dissolution of calcite

A similar approach was used to determine the role of mineral weathering as upwelling CO_2-rich saline water flows through the shallow aquifer. In this case, we modeled the progressive reaction of CO_2-rich saline water (represented by the geyser well) with background water (represented by Well 15), with and without buffering reactions. The results of these calculations are shown in **Figure 10.** Again, we find that the measured trends in pCO_2, Ca, pH, and Cl are fairly well reproduced by this simple model. However, influence of mineral dissolution does not appear to be significant. This is because the CO_2-influsedsaline water is supersaturated with respect to calcite and so as it mixes with background waters it does not necessarily enhance calcite dissolution. Small departures from equilibrium with calcite do occur at specific mixing fractions; these produce the small differences between the solid and dashed lines in **Figure 10**.

Finally, we used PHREEQC to examine a possible explanation for the major ion chemistry measured in the geyser well. We explore the conceptual model proposed by Cumming (1997) of a connate brine rising with CO_2 through the carbonate strata underlying the aquifer. Using a pure Na-Cl brine as a starting composition, we simulated titration with CO_2 in equilibrium with carbonate (calcite and dolomite) until we achieved the pCO_2 measured at the geyser well. Waters were allowed to be slightly supersaturated with respect to carbonate minerals, as is reflected in calculated saturation indices in geyser well samples. By adjusting brine, pH, alkalinity, and target saturation indices, we achieved good agreement between simulated and measured geyser well chemistry, as shown in **Figure 11**. The range of simulated values (bars) represents variation that would be expected due to pCO_2 variation alone. Models assumed brine pH = 12.5, brine [HCO3-] = 1613., SI (calcite) = 0.8, SI (dolomite) = 0.6. Departures from simulated and measured values may be caused by variations other than pCO_2, such as variations in brine chemistry with time or by reactions unaccounted for in this simple model.

Although there are probably other geochemical models that would be equally consistent with the measured water chemistry data, the very simple models we have tested are generally consistent with observed trends at this site and known aquifer mineralogy found in this area. We conclude that when CO_2 diffuses through the aquifer, it reaches higher levels in some locations than in others due to geologic heterogeneity, hydrodynamic factors, and/or spatial variations in CO_2 flux. Mineral weathering is sufficiently rapid relative to the CO_2 flux rate so as to prevent pH from lowering below 6.2 in the vast majority of samples (note: during one sampling round reported by Cumming (1997) somewhat lower values (down to 5.8) were reported in 3 wells). In contrast, when CO_2 upwells along with saline water, the reactivity of the solution is low and mineral weathering is inconsequential. Finally, a conceptual model of CO_2-rich connate brine flowing through and dissolving carbonate rocks below the aquifer, as proposed by Cumming (1997), , is quantitatively consistent with measured values of major ion concentrations at the geyser well.

Impact of CO_2 on trace element concentrations

Evidence from measurements and modeling, described above, suggest that there are two distinct mechanisms controlling major ion and stable isotope chemistry at the site: 1) influx of CO_2 and subsequent in-situ mineral weathering and 2) influx of CO_2-rich saline water with relatively little mineral weathering. The two groups of waters can be easily distinguished on the basis of chloride content and carbon isotopes. Recognizing the difference between these two mechanisms is critical for interpretation of trace element concentration data, since mechanism (1) has the potential for mobilizing trace elements *within* the aquifer. This is due to increased levels of CO_2 and depressed pH. Mechanism (2) has the additional potential for transporting trace elements *into* the aquifer. By examination of trace element concentrations in the geyser well (Table 2), it is clear that mechanism (2) has the potential to transport trace elements *into* the aquifer from below. These elevated trace elements are either associated with the connate brine or with carbonate dissolution in layers below the aquifer.

We focus on trace elements possessing known health effects and which were measured at significant concentrations in some of the samples: Fe, U, Pb, As, and F. Variations of trace element concentrations with pCO_2 and chloride are shown in **Figures 12 and 13**. Samples belonging to the two groups (defined based on chloride and carbon isotopes) are indicated by symbols: mechanism (1) (solid symbols) and mechanism (2) (open symbols). Although our sample size is too small to allow statistically robust comparisons, several notable trends are evident. As, U, and Pb and Fe are all significantly enriched in the high chloride waters; in fact, by examination of **Figure 13** it is clear that As, U, and Pb increase linearly with chloride in this group. The highest concentrations were measured in the geyser well. This supports the conceptual model for mechanism (2): simple mixing (no reactions) between background groundwater and deeper brackish CO_2-enriched waters, and transport of U, Pb, and As *into* the aquifer from below. For waters inferred to lie along Path 1 of **Figure 4** (mechanism 1), there is no tendency for As, U, or Pb to increase with increasing pCO_2 (**Figure 12**). In fact, the lowest pCO_2 sample has the highest As concentration. In summary, there is no evidence that influx of $[CO_2]$ is changing aquifer conditions so as to release U, Pb, As into groundwater. However, transport of these elements into the aquifer via CO_2-enriched brackish water is a significant source of all three trace elements and represents the greatest risk to drinking water quality at this site.

Trends in measured iron and fluoride are distinct from those described above. With one exception (Well #16), concentration of fluoride tend to be negatively correlated with pCO_2. It is possible that influx of CO_2, and mineral precipitation/dissolution reactions, is causing precipitation or adsorption of fluoride. In a previous study of Chimayó groundwater, Finch (2005) noted a negative correlation between $CaCO_3$ hardness and fluoride. This suggests carbonate dissolution enhanced by CO_2 might be the causative factor. Very high F and As concentrations were measured in a very low pCO_2 well (#15). Here, the pH (8.5) is high enough to cause desorption from anion exchange sites for these two elements (Finch, 2005).

Well 16 has anomalously high levels of both iron and fluoride relative to waters with both higher and lower pCO_2 values. Possibly, reactions are occurring here that are

unique to this site due to local heterogeneity in the aquifer. Local redox conditions might be affecting iron. Regardless, for these two elements it does not appear that either pCO_2-induced reactions or transport into the aquifer from below is controlling concentrations in Chimayó groundwater.

Conclusions and implications for monitoring at a CO_2 sequestration site

From this relatively small sample size at a natural analog site, it is clear that CO_2 is upwelling via at least two pathways; one without significant entrainment of saline water and one with saline water. The latter pathway provides a source of arsenic, uranium, and lead into the aquifer that, while significant, should not be confused with in-situ trace element mobilization. There is no evidence in this dataset that CO_2 is mobilizing arsenic, uranium, or lead within the shallow aquifer. Our geochemical modeling suggests dissolution of calcite prevents significant pH depression and may, therefore, inhibit trace metal mobilization. This is in agreement with reactive-transport modeling studies (Wang and Jaffe, 2004) which predict low or zero enhanced trace metal mobility in buffered, high alkalinity aquifers.

There is *some* indication, however, that CO_2 transport is affecting flouride geochemistry within the aquifer. In this environment, the CO_2-induced pH reduction may be causing fluoride to be adsorbed into aquifer sediments via cation exchange. In aquifers such as this one where naturally-occurring fluoride is a significant hazard locally, CO_2 has a beneficial affect on groundwater quality. There are no clear trends with iron concentrations, which generally tend to be very low in this oxidizing environment.

There are several implications for CO_2 leakage impacts. First, as is evident at the Chimayó site, brine that might either leak directly from the CO_2 reservoir or be entrained into the CO_2 plume as it passes through rocks above the reservoir could have a much greater impact on shallow groundwater quality than the CO_2 itself or by reactions in the aquifer caused by elevated CO_2. As was suggested by Kharaka et al. (2006), consideration of brine co-leakage and/or generation through CO_2-induced dissolution should be an important element of risk assessment. Second, there are a number of factors that could mitigate the impact of CO_2 leakage on shallow groundwater quality and thus make the CO_2 leak difficult or impossible to detect. These include 1) simple mixing and dilution of CO_2-impacted groundwater with ambient groundwater, 2) pH buffering reactions such as calcite dissolution and/or silicate mineral weathering, 3) limited trace metal availability in aquifer minerals, and 4) trace metal scavenging by secondary mineral precipitation. Evaluating the potential importance of the first mechanism, mixing, will require knowledge of the possible mechanisms of leakage (diffuse or focused), the relative magnitude of the leakage flux and ambient groundwater fluxes, and some understanding of local groundwater flow dynamics. Simple calculations and relatively inexpensive site characterization could be very useful for this purpose. Evaluating the potential importance of the buffering reactions due to mineral weathering should also be relatively easy to assess with limited site information. The last two geochemical factors will be very difficult to evaluate without very detailed, site-specific geochemical characterization and even then, the predictive capacity of models may not be adequate for risk assessment purposes. Fortunately, if the first two factors can be shown

to lessen the risk, as appears to be the case in the Chimayó aquifer system, there may be no need to address the more complex and inherently site-specific geochemistry. Conditions favorable for pH depression include a lack of buffering minerals, hydrologic conditions that inhibit mixing and dilution of high CO_2 water (spatially focused, high-flux CO_2), and aquifer heterogeneities that can trap CO_2-enriched water locally and inhibit rapid degassing to the vadose zone. If these conditions exist, very detailed site-specific characterization and monitoring will be critical for any meaningful risk assessment.

List of Figures

List of Tables

Acknowledgements

This work was supported by the US DOE through the Zero Emission Research Technology (ZERT) project. We thank Jim Roberts for access to his wells and to all the

other residents of Chimayó for allowing us to sample their water. We thank Toti Larson, Emily Kluk, Mike Rearick, and George Perkins for their laboratory analyses and discussions on data interpretation. We also gained invaluable insight from discussions with Bill Carey and Dennis Newell.

References

Aiuppa, A., Federico, C., Allard, P., Gurrieri, S., Valenza, M. (2005) Trace metal modeling of groundwater-gas-rock interactions in a volcanic aquifer: Mount Vesuvius, Southern Italy. Chemical Geology 216:289-311.

Anderholm, S.K. (1994) Ground-water recharge near Santa Fe, north-central New Mexico, USGS Water Resources Investigations Report 94-4078. 68 pp.

Baldridge, W.S., Ferguson, J.F., Braile, L.W., Wang, B., Eckhardt, K., Evans, D., Schultz, C., Gilpin, B., Jiracek, G.R., Biehler, S. (1994) The western margin of the Rio Grande Rift in northern New Mexico: An aborted boundary? GSA Bulletin 105:1538-1551.

Benson, S.M. (2002) Lessons learned from natural and industrial analogues for storage of carbon dioxide in deep geological formations. Lawrence Berkeley Laboratory Report, 227pp.

Birkholzer, J., Q. Zhou, Q., J. Rutqvist, J., Jordan, P., Zhang, K., C-F. Tsang, C.-F. (2007) Research project on CO2 geological storage and groundwater resources: Large-scale hydrological evaluation and modeling of the impact on groundwater systems., Annual Report Cot 1, 2006-Sept 30-2007. National Energy Technology Lab.

Birkholzer , J.T. (2008) Prediction of Potential Groundwater Contamination in Response to CO2 Leakage from Deep Geological Storage, 7th Annual Carbon Sequestration Conference: Pittsburgh, PA.

Blake, W.D., Goff, F., Adams, A.I., Counce, D. (1995) Environmental Geochemistry for surface and subsurface waters in the Pajarito Plateau and outlying areas, New Mexico, Los Alamos National Laboratory Report, 43pp.

Bose, P., Sharma, A. (2002) Role of iron in controlling speciation and mobilization of arsenic in subsurface environment. Water Research 36:4916-4926.

Bruno, J., Stumm, W., Wesin, P., Bandberg, F. (1992) On the influence of carbonate in mineral dissolution: I. the thermodyamics and kinetics of hematite dissolution in bicarbonate solutions at T=25°C. Geochimica et Cosmochimica Acta 56:1139-1147.

Cavazza, W. (1986) Miocene Sediment Dispersal in the Central Espanola Basin, Rio Grande Rift, New Mexico, USA. Sedimentary Geology 5:119-135.

Chen, Z. (2005) In situ feldspar dissolution rates in an aquifer. Geochimca et Cosmochimica Acta 69:1435-1453.

Craw, D., Falconer, D., Youngson, J.H. (2003) Environmental arsenopyrite stability and dissolution: theory, experiment, and field observations. Chemical geology 199:71-82.

Cumming, K.A., 1997, Hydrogeochemistry of groundwater in Chimayo, New Mexico M.S., Northern Arizona University, Flagstaff, AZ.

Evans, W.C., Sorey, M.L., Cook, A.C., Kennedy, B.M., Shuster, D.L., Colvard, E.M., White, L.D., Huebner, M.A. (2002) Tracing and quantifying magmatic carbon discharge in cold groundwaters: Lessons learned from Mammoth Mountain, USA. Journal of Volcanology and Geothermal Research 114:291-312.

Federico, C., Aiuppa, A., Favara, R., Gurrieri, S., Valenza, M. (2004) Geochemical monitoring of groundwaters (1998-2001) at Vesuvius volcano (Italy). Journal of Volcanology and Geothermal Research 133:81-104.

Finch, S.T. (2005) Occurrence of Elevated Arsenic and Fluoride Concentrations in the Española Basin, *in* McKinney, K.C., ed., 4th Annual Española Basin Workshop: Santa Fe, New Mexico, U.S.Geological Survey, p33.

Gallaher, B.M., Efurd, D.W., Steiner, R.E. (2004) Uranium in waters near Los Alamos National Laboratory: concentrations, trends, and isotopic composition through 1999, Los Alamos National Laboratory, 70pp.

Glennon, J.A.a.P.R.M. (2005) The operation and geography of carbon-dioxide-driven, cold-water geysers. GOSA Transactions 9:184-192.

Goff, F., Shevenell, L., Gardner, J.N., Vuataz, F.D., Grigsby, C.O. (1988) The hydrothermal outflow plume of Valles Caldera, New Mexico, and a comparison with other outflow plumes. J.Geophys.Res. 93:6041-6058.

Golubev, S.V., Pokrovsky, O.S., Schott, J. (2005) Experimental determination of the effect of dissolved CO2 on the dissolution kinetics of Mg and Ca silicates at 25°C. Chemical geology 217:227-238.

Hereford, A.G., Keating, E., Guthrie, G.D., Zhu, C. (2007) Reactions and reaction rates in the regional aquifer beneath the Pajarito Plateau, north-central New Mexico, USA. Environmental Geology 52:965-977.

Keating, E., Warren, R. (1999) Geochemistry of the regional aquifer, Los Alamos National Laboratory Report 35pp.

Kharaka, Y.K., Cole, D.R., Hovorka, S., Gunter, W.D., Knauss, K.G., Freifeld, B.M. (2006) Gas-water-rock interactions in Frio Formation following CO2 injection: Implications for the storage of greenhouse gases in sedimentary basins. Geology 34:577-580.

Koning, D.J., Skotnicki, S., Nyman, M., Horning, R., Eppes, M., and Rogers, S. (2002) Geology of the Cundiyo 7.5-minute quadrangle, Santa Fe County, New Mexico: New Mexico Bureau of Geology and Mineral Resources, Open-file Geologic Map OF-GM-56, scale 1:24,000.

Koning, D.J. (2003) revised Dec-2005, Geologic map of the Chimayo 7.5-minute quadrangle, Rio Arriba and Santa Fe Counties, New Mexico: New Mexico Bureau of Geology and Mineral Resources, Open-file Geologic Map OF-GM-71, scale 1:24,000.

Langmuir, D. (1997) Aqueous Environmental Chemistry: Upper Addle River, New Jersey, Prentice-Hall, Inc, 600 pp.

Liewicki, J.L., Birkholzer , J.T., Tsang, C.-F. (2007) Natural and industrial analogues for leakage of CO2 from storage reservoirs: identification of features, events, and processes and lessons learned. Environmental Geology 52:457-467.

Lu, X., Watson, A., Gorin, A.V., Deans, J. (2005) Measurements in a low temperature CO2-driven geysering wel, viewed in relation to natural geysers. Geothermics 34:389-410.

McQuillan, D., Montes, R. (1998) Ground-water geochemistry, Pojoaque Pueblo, New Mexico: Santa Fe, NM, New Mexico Environment Department, 34pp.

Mook, W.G., Bommerson, J.C., Staverman, W.H. (1974) Carbon Isotope Fractionation between dissolved bicarbonate and gaseous carbon dioxide. Earth and planetary science letters 22:169-176.

Newell, D., Crossey, L.J., Karlstrom, K.E., Fischer, T.P. (2005) Continental-scale links between the mantle and groundwater systems of the western United States: Evidence from travertine springs and regional He isotope data. GSA Today 15:4-10.

New Mexico Environment Department (1980) Chemical quality of New Mexico Community Water Supplies, Volume 1980, Water Supply Section

Purtymun, W.D. (1977) Hydrologic characteristics of the Los Alamos Well field, with reference to the occurrence of arsenic in well LA-6, Los Alamos National Laboratory Report, p. 63.

Rogers, D.B., Stoker, A.K., McLin, S.G., Gallaher, B.M., 1996, Recharge to the Pajarito Plateau regional aquifer system, NM Geol.Soc.Guidebook, 47th Field conference, Jemez Mountins Region, p. 407-412.

Rogie, J.D., Kerrick, D.M., Sorey, M.L., Chiodini, G., Galloway, D.L. (2001) Dynamics of carbon dioxide emission at Mammoth Mountain, California. Earth and planetary science letters 188:535-541.

Smyth, R.C., Holtz, M.H., Guillot, S.N. (2006) Assessing Impacts to Groundwater from CO_2-flooding of SACROC and Claytonville Oil Fields in West Texas. presented at the 2006 UIC Conference of the Groundwater Protection Council, Austin, Texas, January 24, 2006.

Stephens, J.C., Hering, J.G. (2004) Factors affecting the dissolution kinetics of volcanic ash soils: dependencies on pH, CO2, and oxalate. Applied Geochemistry 19:1217-1232.

Street, J.B., Finch, S. (2004) Well report Buckman wells no. 10 through 13, City of Santa Fe, New Mexico: Albuquerque, N.M., John Shomaker and Associates, Inc., p. 59

U.S. Geological Survey (1997) WATSTORE database, Volume 1997 retrieval.

Vuataz, F.D., Goff, F., Fouillac, C., Calvez, J.Y. (1986) Isotope geochemistry of thermal and nonthermal waters in the Valles Caldera, Jemez Mountains, northern New Mexico. J. Geophysics Res. 91:1835-1853.

Vuataz, F.D., Stix, J., Goff, F., Pearson, C.F. (1984) Low-temperature geothermal potential of the Ojo Caliente warm springs area, northern New Mexico, Los Alamos National Laboratory Report, 56pp.

Wang, S., Jaffe, P.R. (2004) Dissolution of a mineral phase in potable aquifers due to CO2 releases from deep formations; effect of dissolution kinetics. Energy conversion and management 45:2833-2848.

Table 1. Major Ion concentrations (mg/l)

Well	Ca	Cl	Fe	HCO_3	K	Mg	Mn	Na	NO_3	SiO_2	SO_4	TDS	pH	pCO_2*
17	527.2	647.5	1.71	2975.0	40.4	207.2	1.546	1141.5	<0.01	76.4	259.0	5890.8	6.4	0.0
3	122.6	22.0	0.02	500.2	3.8	21.4	<0.001	13.4	1.0	18.7	14.2	721.4	7.0	-1.3
1	74.2	5.3	0.01	289.0	1.9	5.6	0.090	8.2	1.3	17.0	8.9	412.6	7.0	-1.6
2	105.2	72.5	0.01	670.0	4.0	10.3	0.289	145.0	1.5	20.8	106.0	468.1	6.4	-0.6
5	179.5	22.1	0.26	1096.0	6.3	33.1	0.716	116.4	<0.01	29.2	43.7	1535.2	6.5	-1.1
7	135.2	23.1	0.04	703.0	5.2	22.4	0.004	75.5	3.3	23.9	49.4	1046.0	6.9	-1.1
8	91.8	11.4	<0.01	371.0	1.5	10.5	0.001	18.3	3.1	27.2	15.7	554.7	7.1	-1.7
6	127.4	12.6	0.01	549.9	3.1	15.9	<0.001	26.3	1.0	16.8	17.9	775.2	6.8	-0.5
4	85.2	7.7	0.03	403.0	3.1	14.8	0.053	22.1	0.4	15.7	20.3	575.2	7.1	-1.5
9	314.2	372.0	<0.01	1903.0	16.0	57.0	1.692	602.6	1.0	60.8	261.0	2961.8	6.3	-0.1
10	86.2	14.4	<0.01	387.7	1.7	6.2	0.003	39.8	2.6	37.0	28.0	560.7	7.4	-1.9
11	98.3	10.6	<0.01	380.2	1.8	8.0	0.004	16.2	3.6	19.2	14.9	525.3	7.2	-1.7
12	74.3	11.8	0.01	336.5	2.1	8.0	0.101	24.8	0.1	23.6	16.8	470.3	6.8	-1.3
13	86.2	3.4	<0.01	356.5	1.1	10.4	0.012	12.2	1.6	28.1	9.3	495.9	7.3	-1.8
14	99.6	15.2	<0.01	382.0	1.6	11.1	0.003	18.9	4.7	26.7	18.0	542.2	7.7	-2.1
15	6.7	33.2	0.03	178.7	0.7	0.2	0.003	94.0	5.6	12.4	49.6	301.1	8.5	-3.3
16	308.0	279.3	<0.01	1377.9	11.8	30.9	2.460	435.1	0.1	47.6	232.7	2217.6	6.3	-0.2

- calculated using PHREEQC

Table 2. Trace element concentrations (mg/l)

Well	Ag	Al	As	B	Ba	Cr	Cu	F	Pb	Ni	Sr	U	V	Zn
17	0.002	<0.002	0.019	1.593	<0.05	<0.05	<0.05	<0.01	0.0104	<0.05	7.649	0.157	<0.05	0.043
3	<0.001	0.006	0.001	0.027	0.701	0.031	0.028	0.385	0.0002	0.004	2.710	0.023	0.010	0.021
1	<0.001	0.010	0.000	0.026	0.394	0.003	0.025		<0.0002	0.003	0.550	0.004	0.009	0.003
2	<0.001	0.027	0.002	0.127	0.074	0.013	0.078	0.250	0.0025	0.005	0.776	0.045	0.022	0.080
5	<0.001	0.019	0.001	0.115	0.141	0.009	0.002	2.120	<0.0002	0.009	2.877	0.014	0.019	0.064
7	<0.001	0.016	0.002	0.081	0.147	0.006	0.009	1.570	<0.0002	0.005	1.944	0.044	0.020	0.083
8	0.002	0.011	0.002	0.072	0.277	0.003	0.392	1.250	0.0002	0.004	1.152	0.016	0.012	0.054
6	0.001	0.011	0.003	0.048	0.652	0.005	0.161	0.710	0.0025	0.006	1.968	0.016	0.016	0.153
4	<0.001	0.008	0.000	0.031	0.178	0.004	0.004	0.738	<0.0002	0.004	1.667	0.029	0.010	0.058
9	<0.001	0.035	0.007	0.582	0.035	0.031	0.122	0.376	0.0033	0.075	3.088	0.048	0.058	0.769
10	<0.001	0.001	0.003	0.032	0.232	0.005	1.044	1.629	0.0005	0.012	0.537	0.013	0.014	0.223
11	0.005	0.011	0.001	0.016	0.374	0.005	0.108	0.845	0.0020	0.007	0.818	0.012	0.014	0.205
12	<0.001	0.003	0.000	0.024	0.137	0.004	0.011	0.959	0.0001	0.005	0.649	0.013	0.009	0.018
13	<0.001	0.001	0.001	0.020	0.339	0.005	0.006	0.923	0.0001	0.006	0.878	0.028	0.015	0.060
14	0.002	0.004	0.002	0.022	0.542	0.005	0.272	0.955	0.0014	0.007	1.056	0.015	0.017	0.275
15	0.003	0.003	0.014	0.133	0.025	0.006	0.058	6.595	0.0013	<0.001	0.169	0.033	0.020	0.028
16	<0.001	0.007	0.002	0.434	0.041	0.022	0.013	3.848	0.0001	0.021	2.468	0.015	0.039	0.012

Table 3. Stable isotope concentrations

Well		δD (‰)	$\delta^{18}O$ (‰)	$\delta^{13}C$ (‰)
17 (water)	4/2007	-91.91	-11.4[1]	3.8[2]
17 (water)	1997[3]	-	-	-0.55
17 (gas)	1997[3]	-	-	-7.11
7	7/2008	-87.14	-11.3[2]	-4.2[2]
8	7/2008	-87.01	-11.87	-12.5
6	7/2008	-86.20	-11.67	-8.8[2]
4	7/2008	-84.54	-11.64[2]	-12.4[2]

9	7/2008	-90.34	-11.20	4.32
10	7/2008	-84.30	-11.37	-11.18
11	7/2008	-86.52	-11.76	-11.53
12	7/2008	-87.95	-11.96	-6.87
13	7/2008	-84.59	-11.47	-12.59
14	7/2008	-88.77	-11.92	-12.31[2]
15	7/2008	-97.28	-12.85	-8.95
16	4/2007	-90.99	-11.57[1]	0.97
16	7/2008	-91.37	-11.49[2]	5.36

[1]average of three replicates
[2]average of two replicates
[3]Cumming (1997)

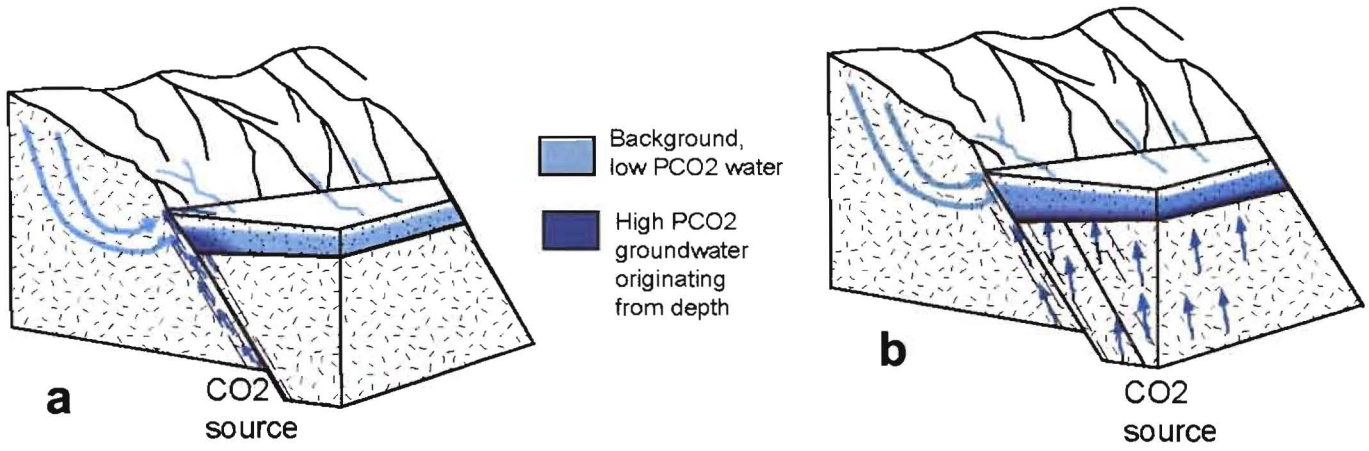

Figure 1. Two types of natural analogs a) CO_2 rises with deep water along a fault and forms a CO_2-rich spring b) CO_2 rises with deep water along a faults and diffuses into shallow aquifer water. CO_2 degasses at springs and also along the water table to the vadose zone.

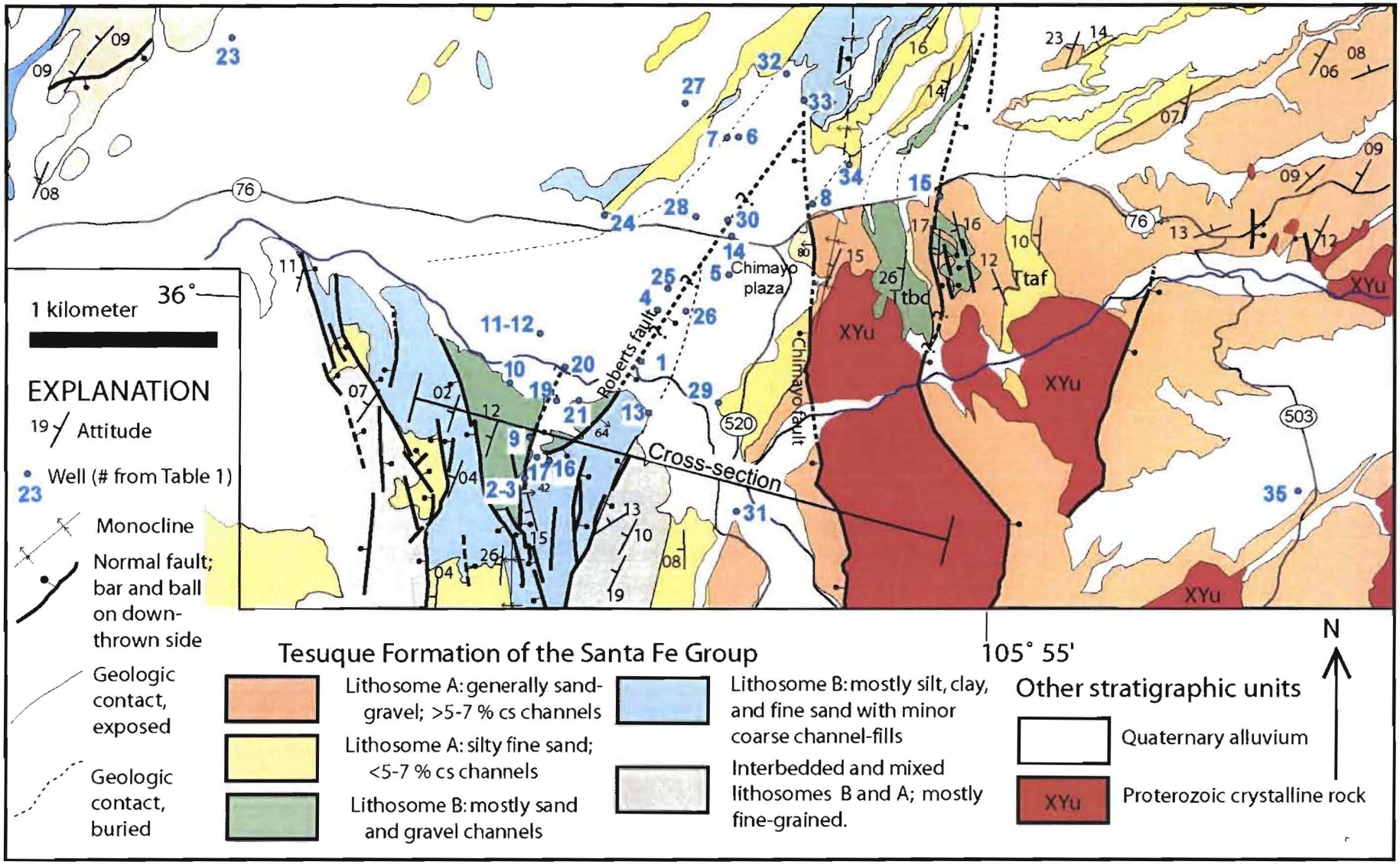

Figure 2. Map of Chimayo showing surface geology and well locations. (Koning et al., 2002; Koning, 2003)

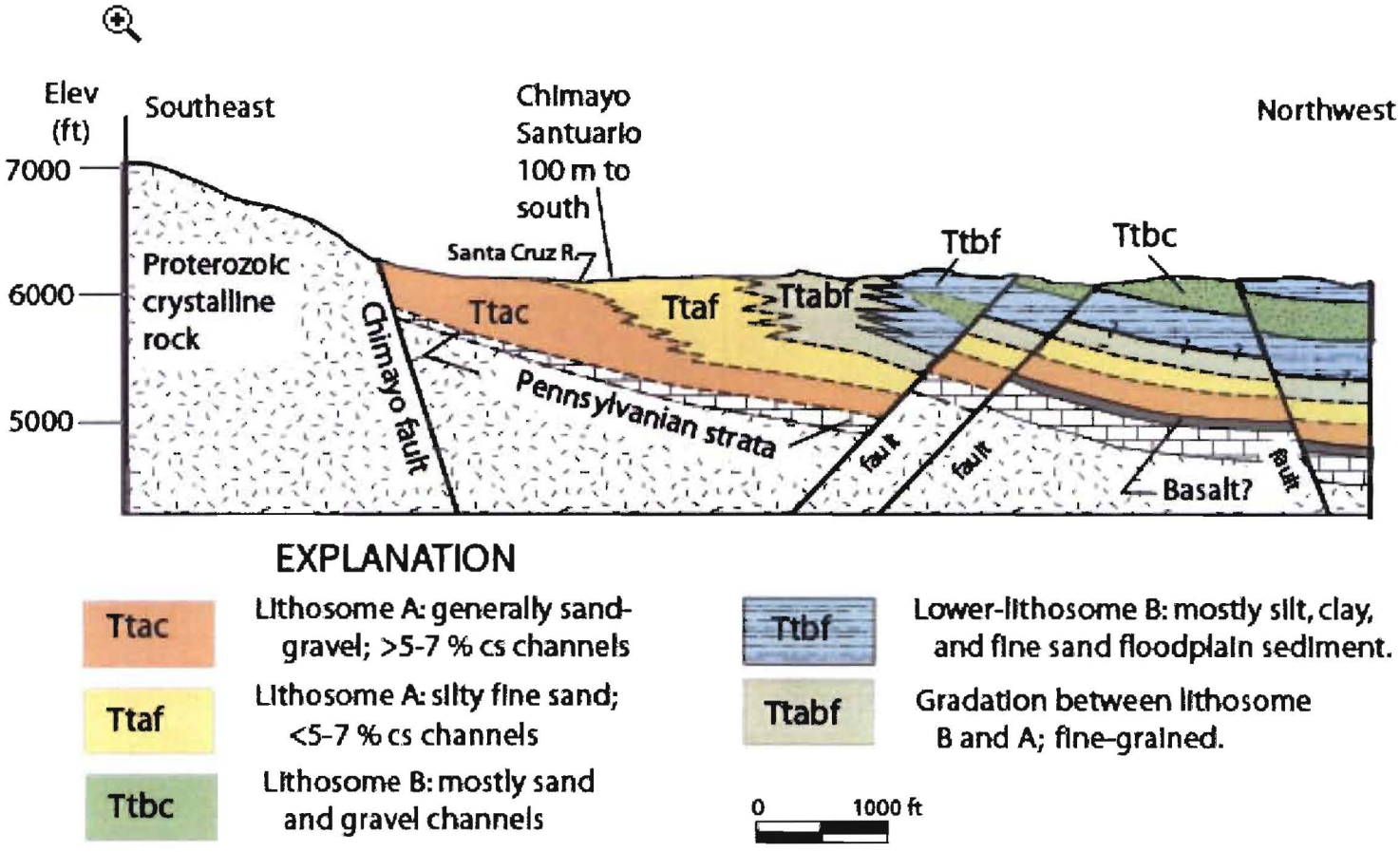

Figure 3. Cross-section through Chimayo; location of section shown on Figure 2 (Koning et al., 2002; Koning, 2003)

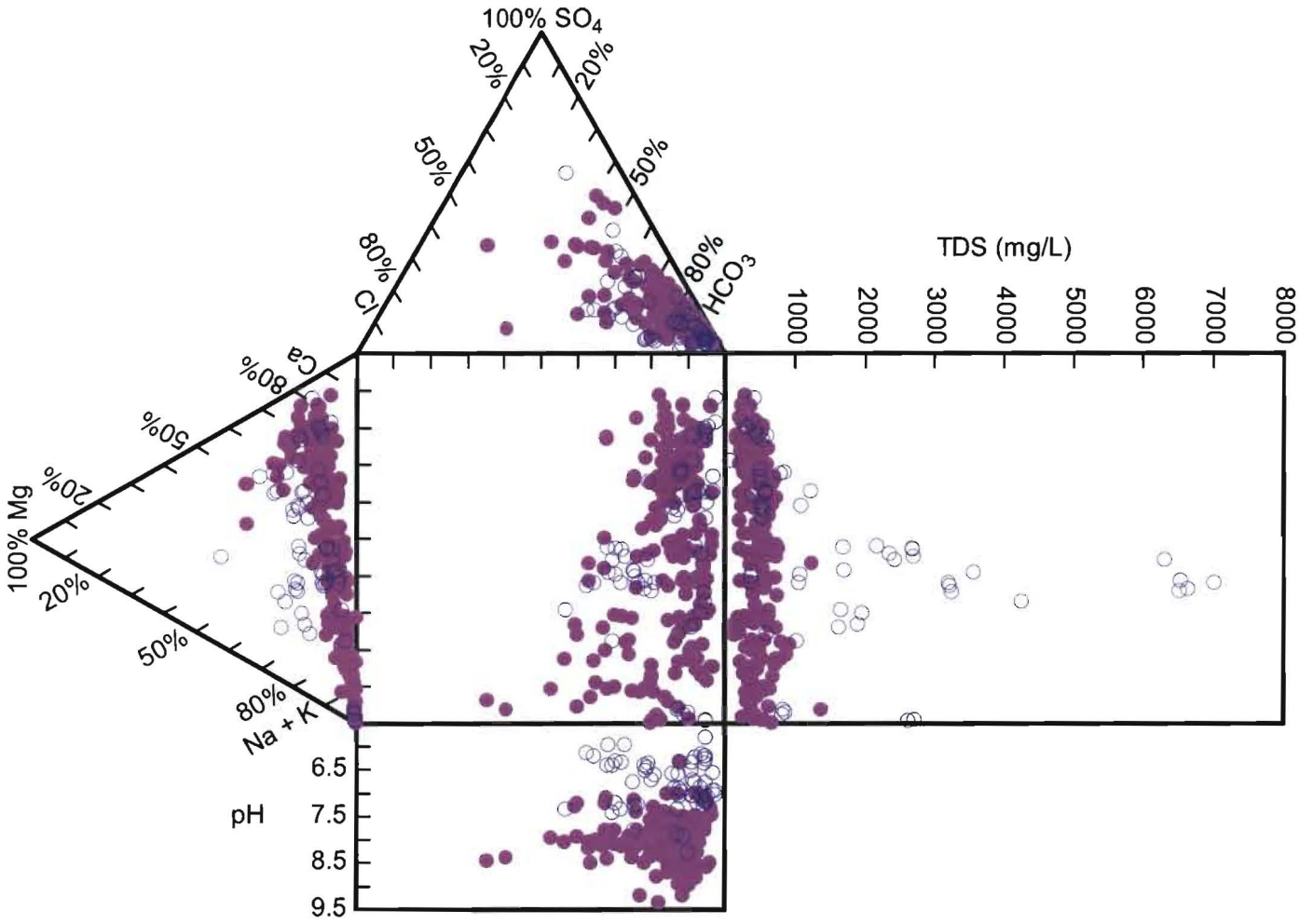

Figure 4. Durov diagram, indicating major ion chemistry, pH, and TDS of groundwater in the Espanola Basin, east of the Rio Grande (pink symbols), in comparison to groundwater in the Chimayo area (blue symbols).

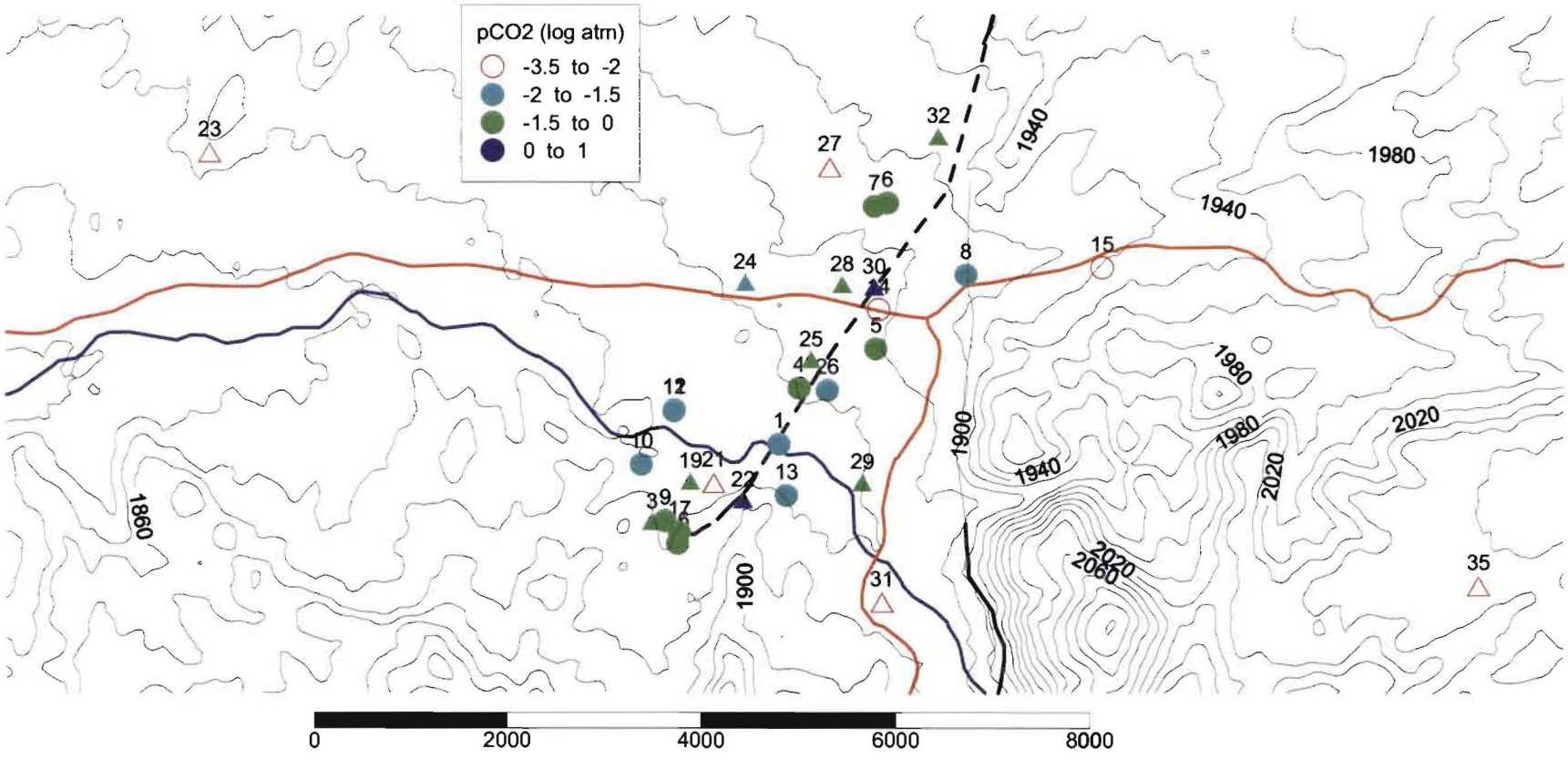

Figure 5a. Variation in pCO_2 in Chimayo groundwaters (data from this study (circles) and Cummings (1997) (triangles))

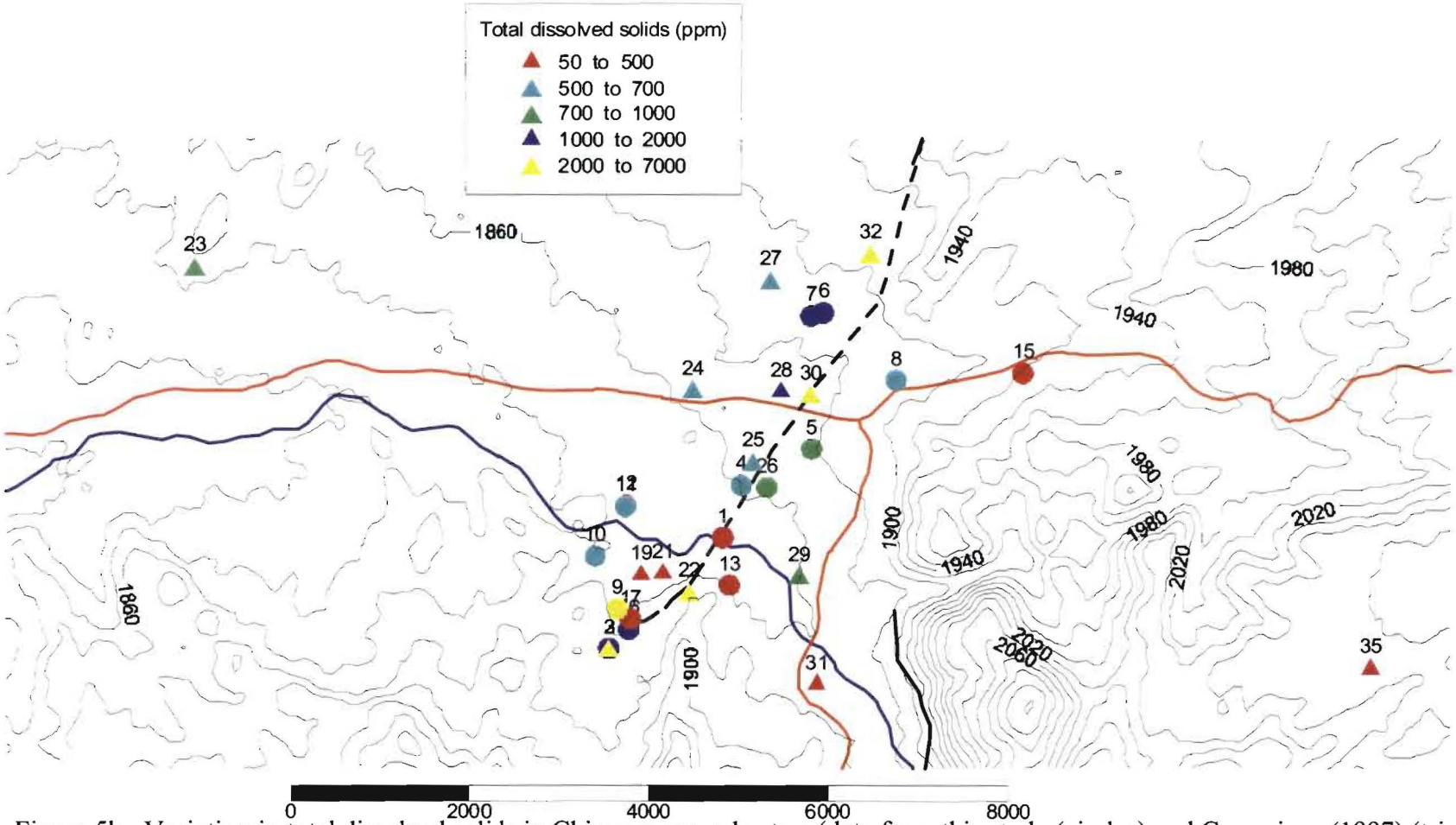

Figure 5b. Variation in total dissolved solids in Chimayo groundwaters (data from this study (circles) and Cummings (1997) (triangles))

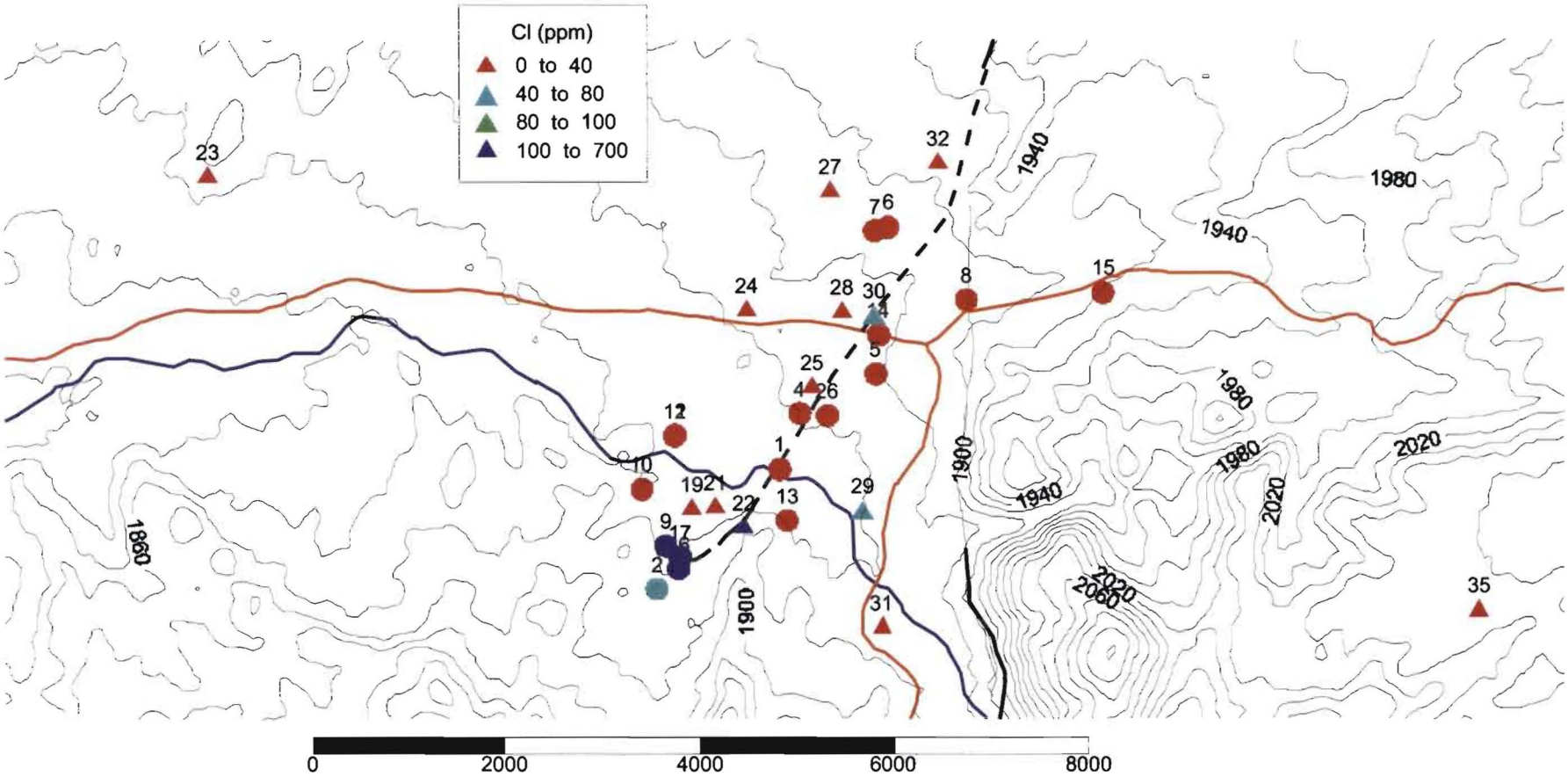

Figure 5c. Variation in chloride concentrations in Chimayo groundwaters (data from this study (circles) and Cummings (1997) (triangles))

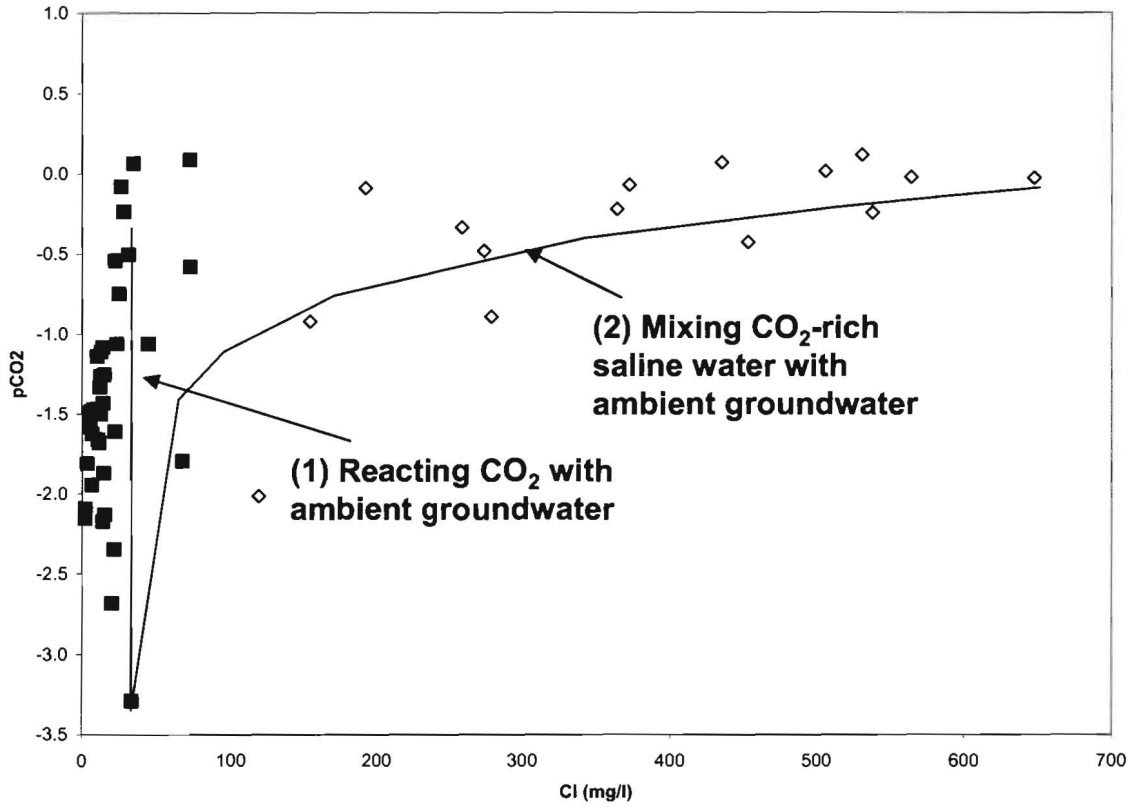

Figure 6. Variation of chloride and pCO_2 in Chimayo waters. Solid lines refer to two proposed mixing/geochemistry models, described in text. Open symbols ([Cl]> 100mg/l); closed symbols ([Cl] < 100mg/l).

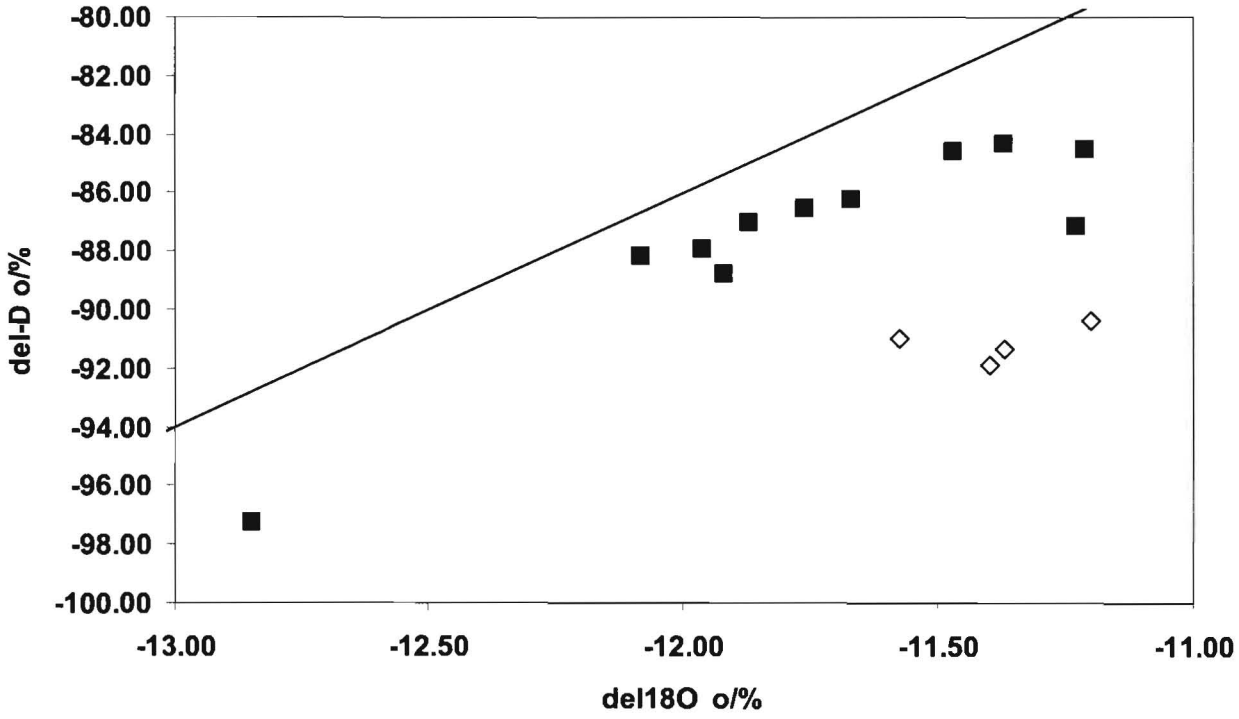

Figure 7. Variation in $\delta^{18}O$ ‰ and δD ‰ in Chimayo groundwater. World meteoric line is shown for comparison. Open symbols ([Cl]> 100mg/l); closed symbols ([Cl] < 100mg/l).

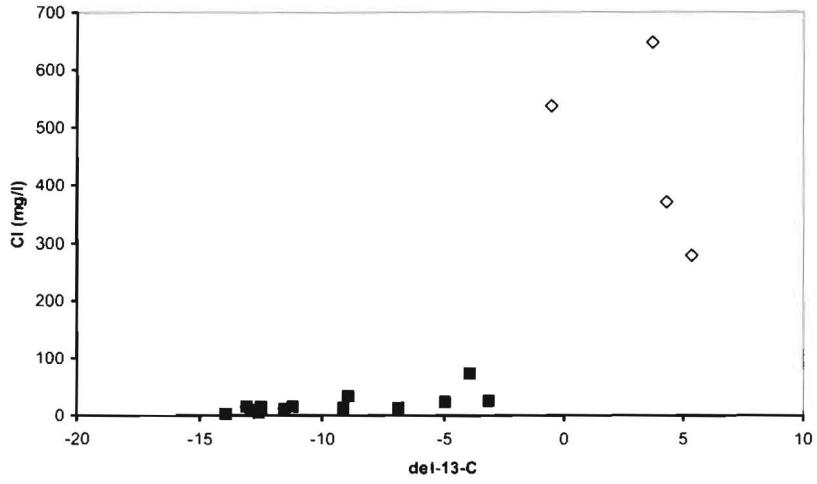

a

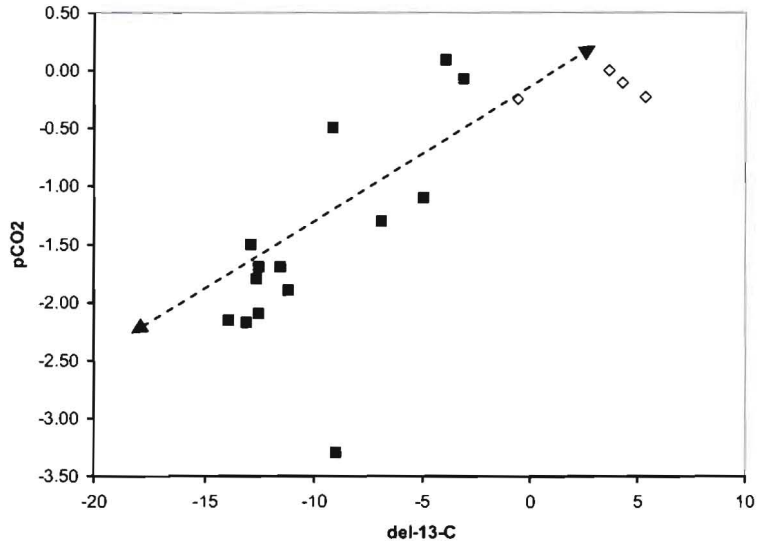

b

Figure 8. Variation in a) Cl and b) pCO2 with respect to δ13C in Chimayo groundwater. Open symbols ([Cl]> 100mg/l); closed symbols ([Cl] < 100mg/l).

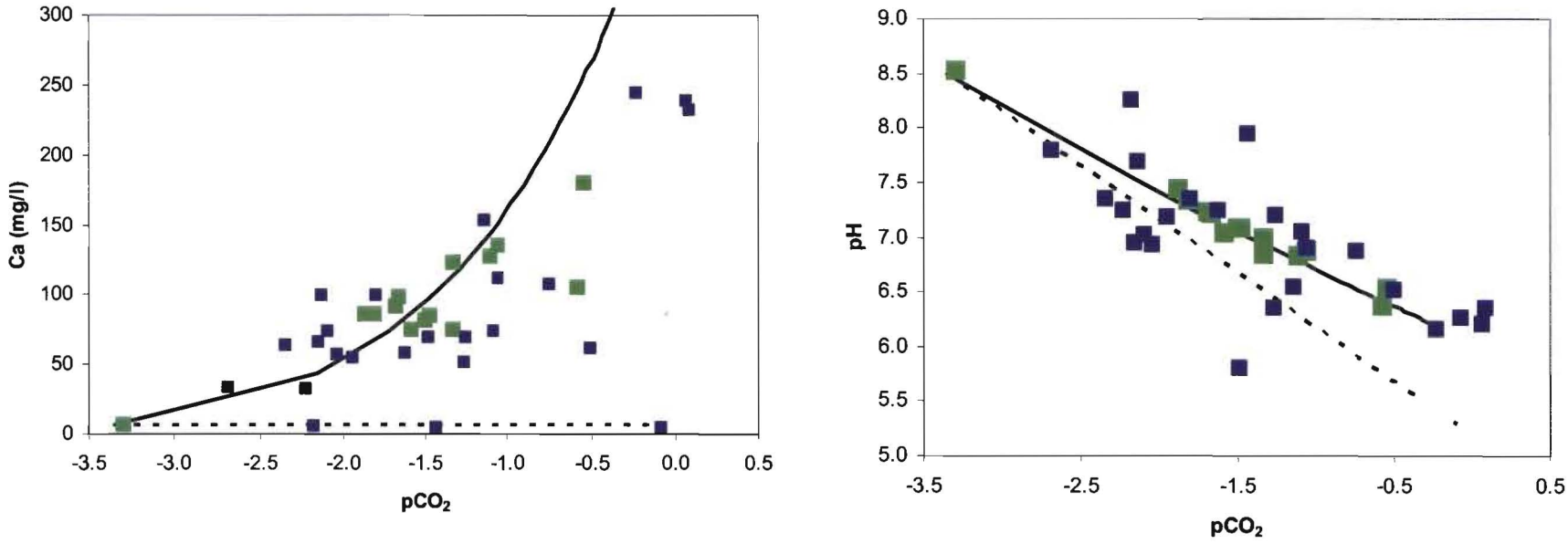

Fig. 9. PHREEQC simulations of background waters reacting with CO_2 in equilibrium with calcite compared to measured values of pCO_2, pH, and Ca for all groundwaters with [Cl] < 100 mg/l. Solid lines are Model A, dotted lines are Model B. Blue symbols are data reported by Cumming (1997); green symbols are data collected in this study.

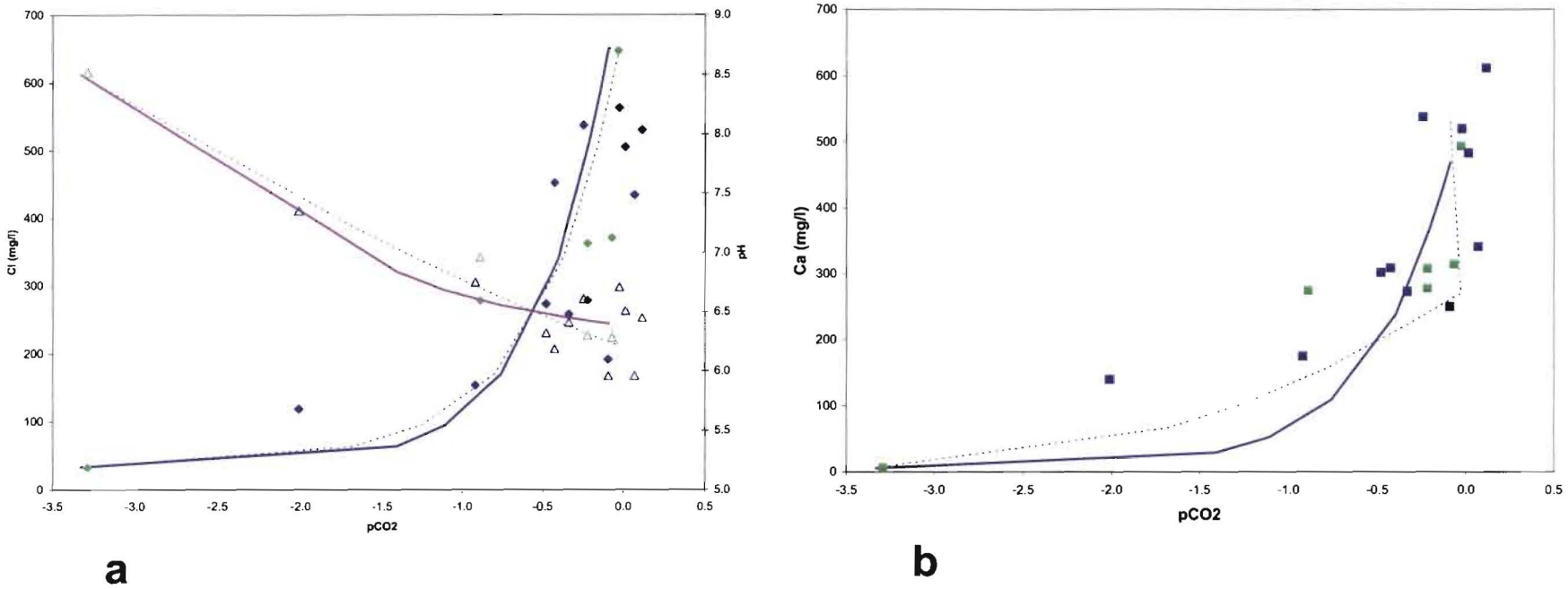

Fig. 10. PHREEQC simulations of background waters mixing with CO_2 and saline water (represented by the geyser sample) compared to water samples with [Cl]>100 mg/l. Solid lines represent mixing and aqueous reactions; dotted lines include calcite dissolution. Blue symbols are data reported by Cumming (1997); green symbols are data collected in this study. a) measured pH (triangles) and simulated pH (pink lines), measured [Cl] (diamonds) and simulated [Cl] (blue lines); b) measured and simulated [Ca]

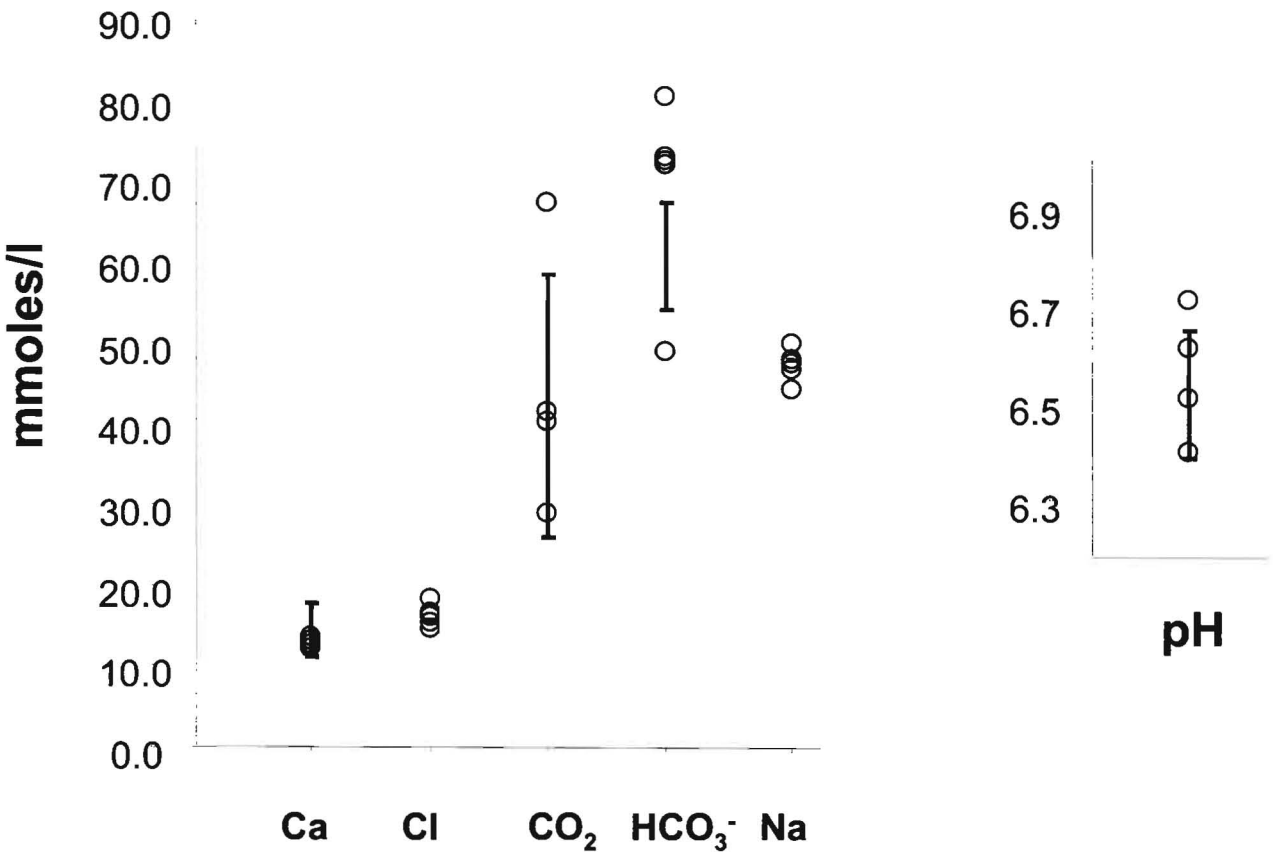

Figure 11. Measured concentrations of major ions in the geyser well (open symbols). Range of simulated values (bars).

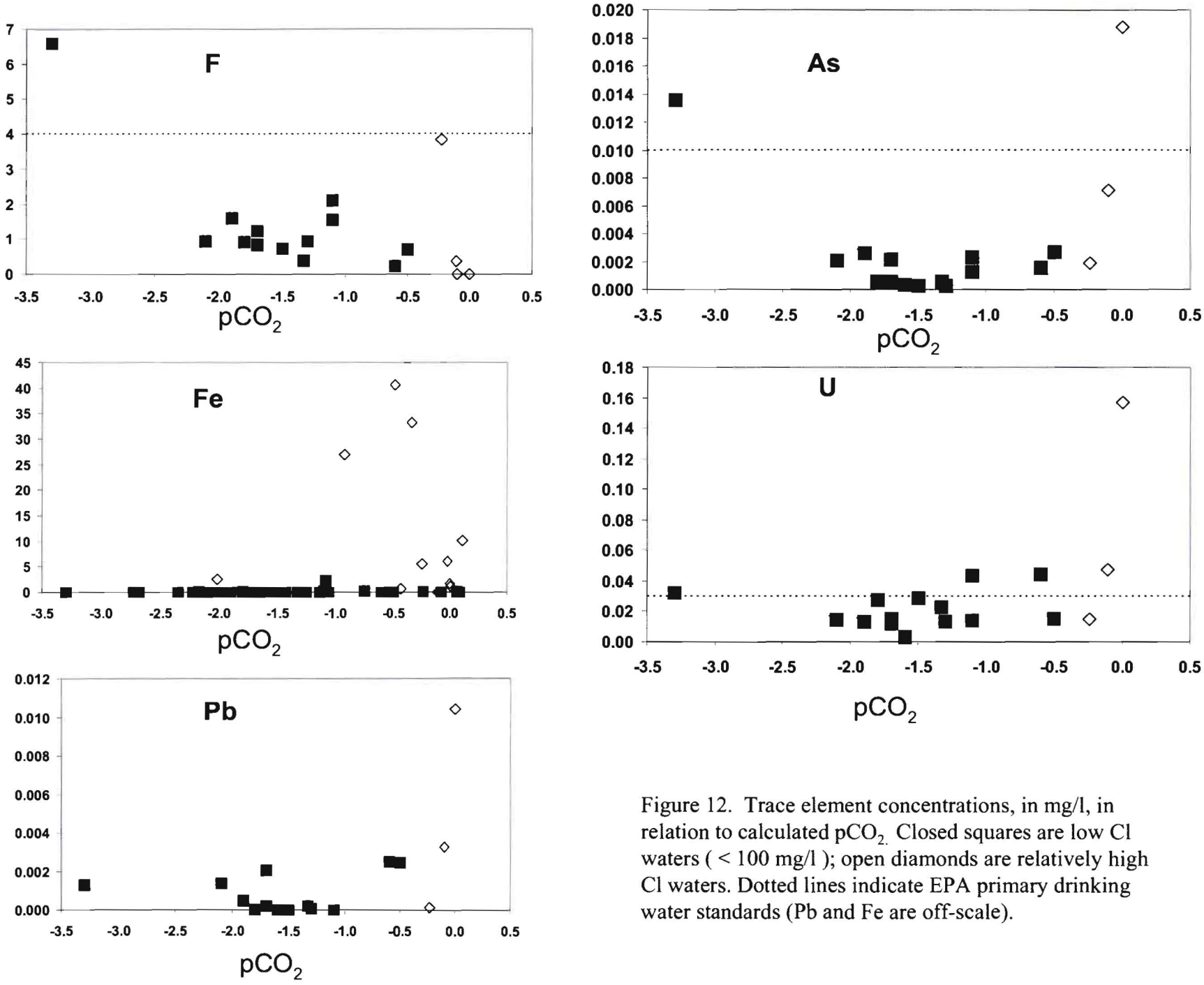

Figure 12. Trace element concentrations, in mg/l, in relation to calculated pCO_2. Closed squares are low Cl waters (< 100 mg/l); open diamonds are relatively high Cl waters. Dotted lines indicate EPA primary drinking water standards (Pb and Fe are off-scale).

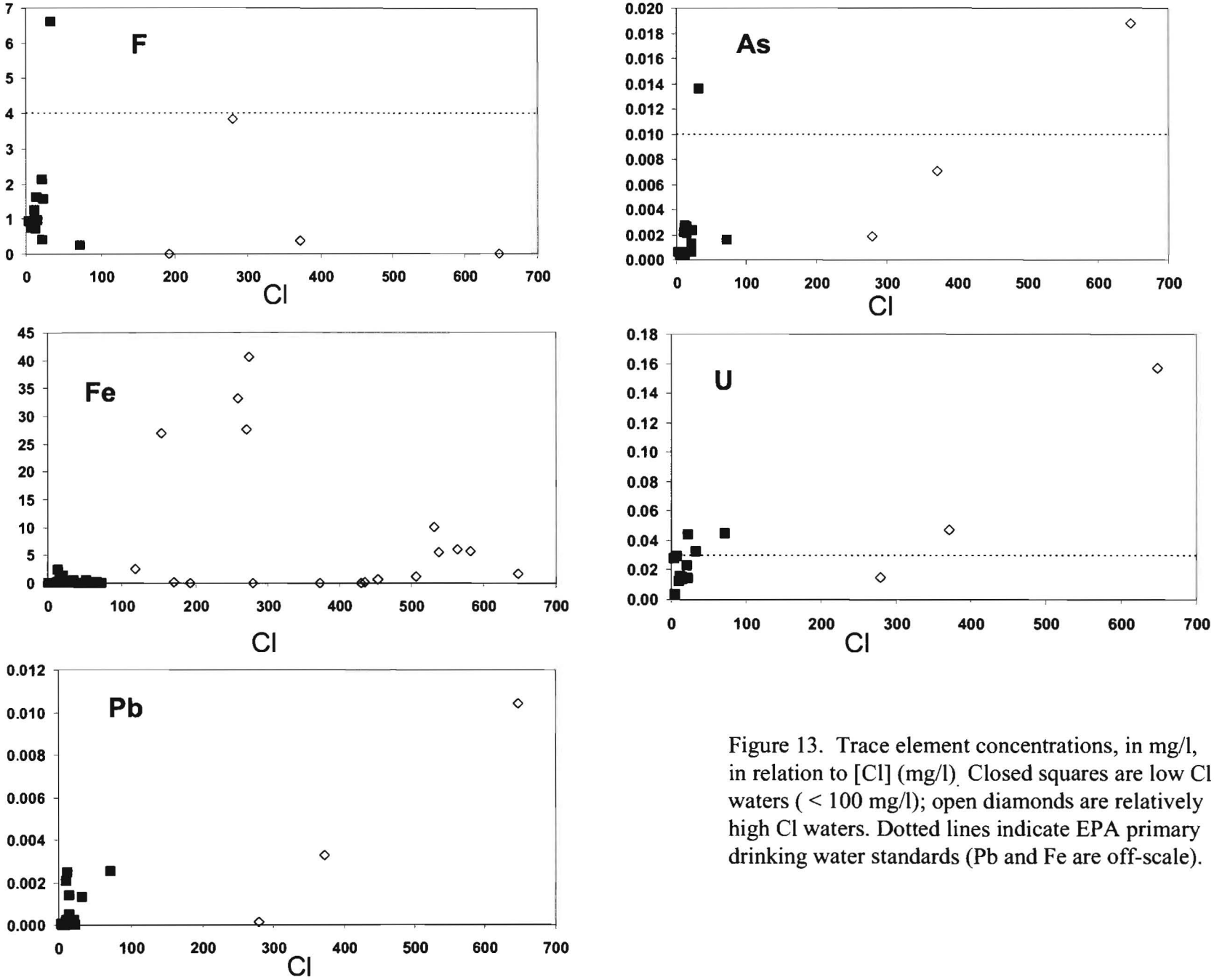

Figure 13. Trace element concentrations, in mg/l, in relation to [Cl] (mg/l). Closed squares are low Cl waters (< 100 mg/l); open diamonds are relatively high Cl waters. Dotted lines indicate EPA primary drinking water standards (Pb and Fe are off-scale).

Supplementary material

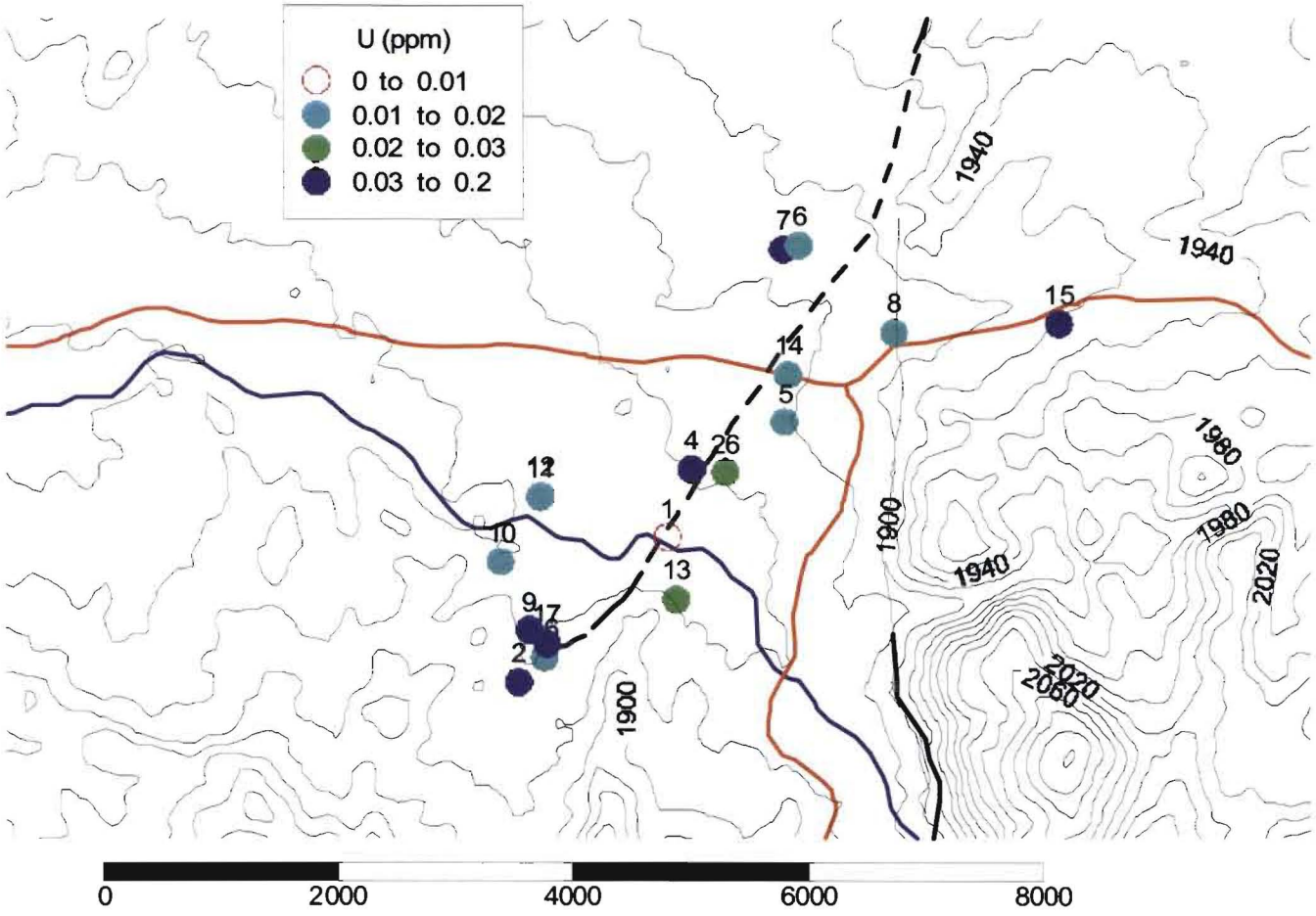

Uranium concentrations

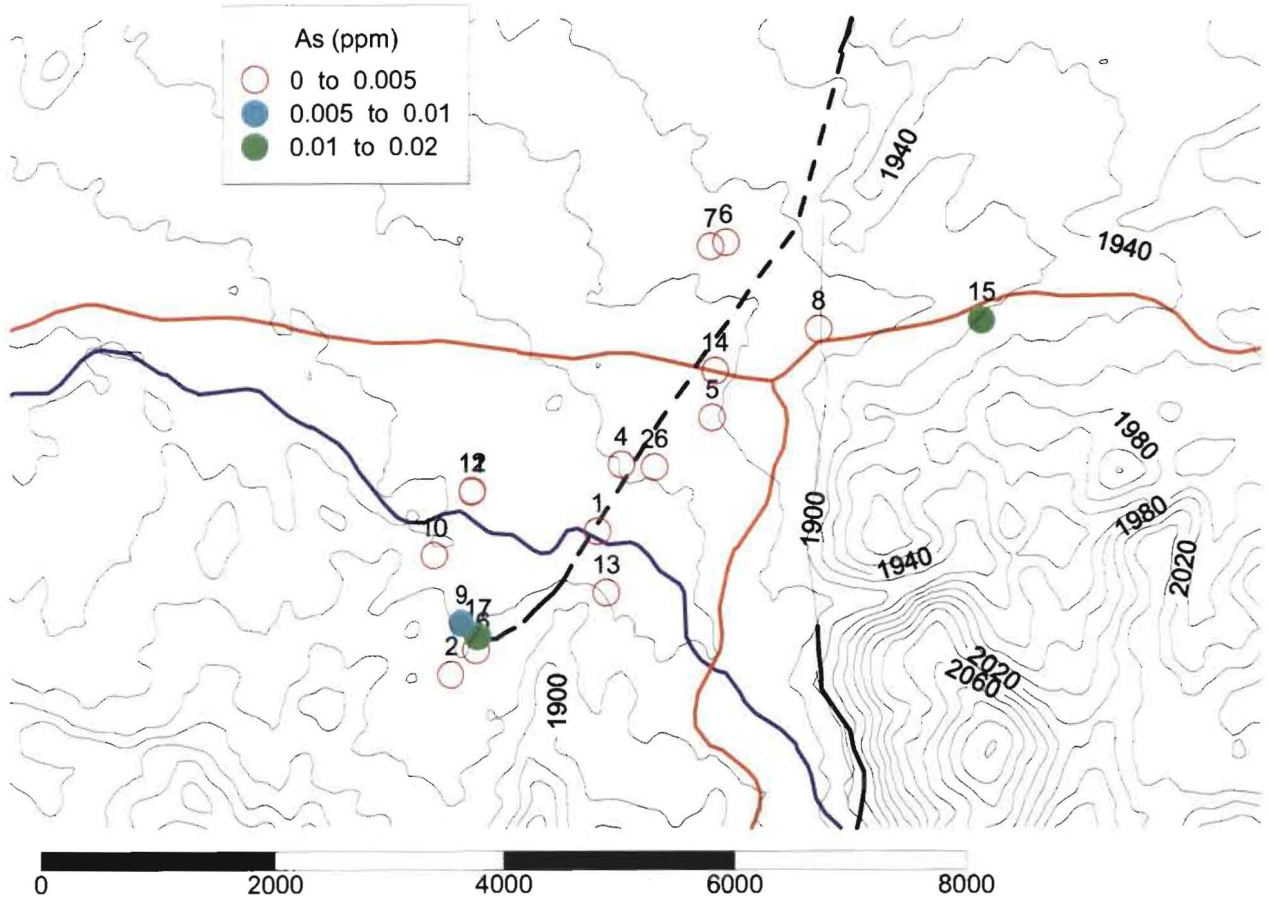

Arsenic concentrations

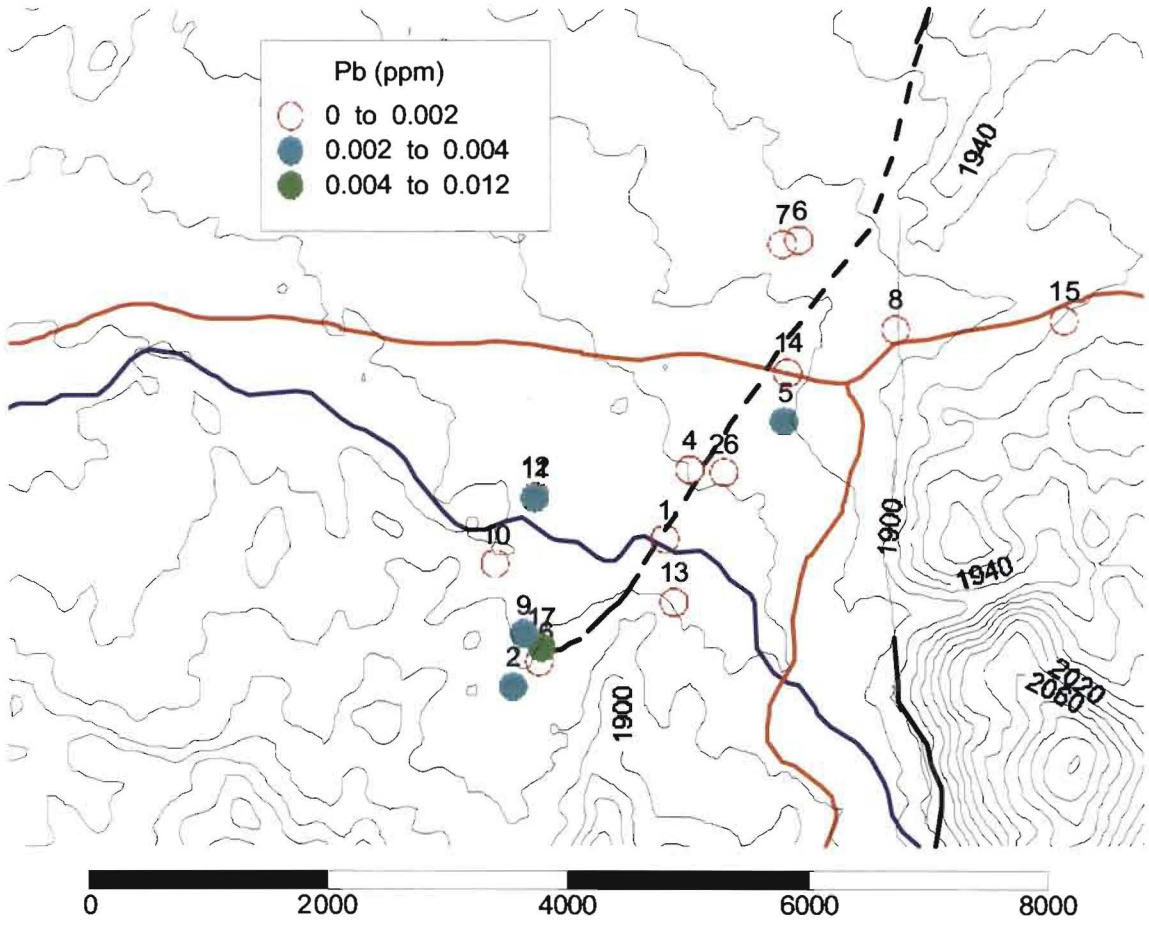

Lead concentrations

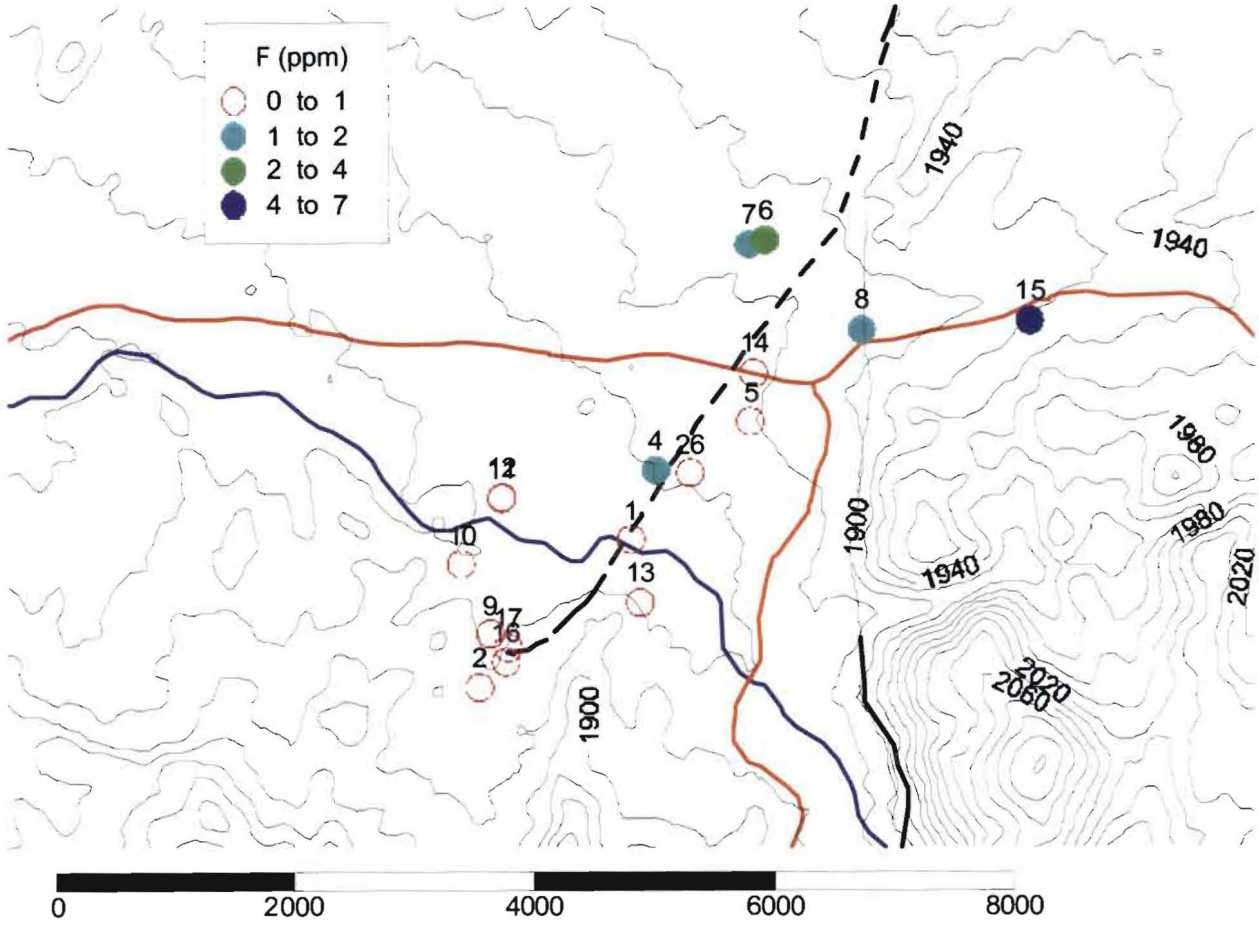

Flouride concentrations

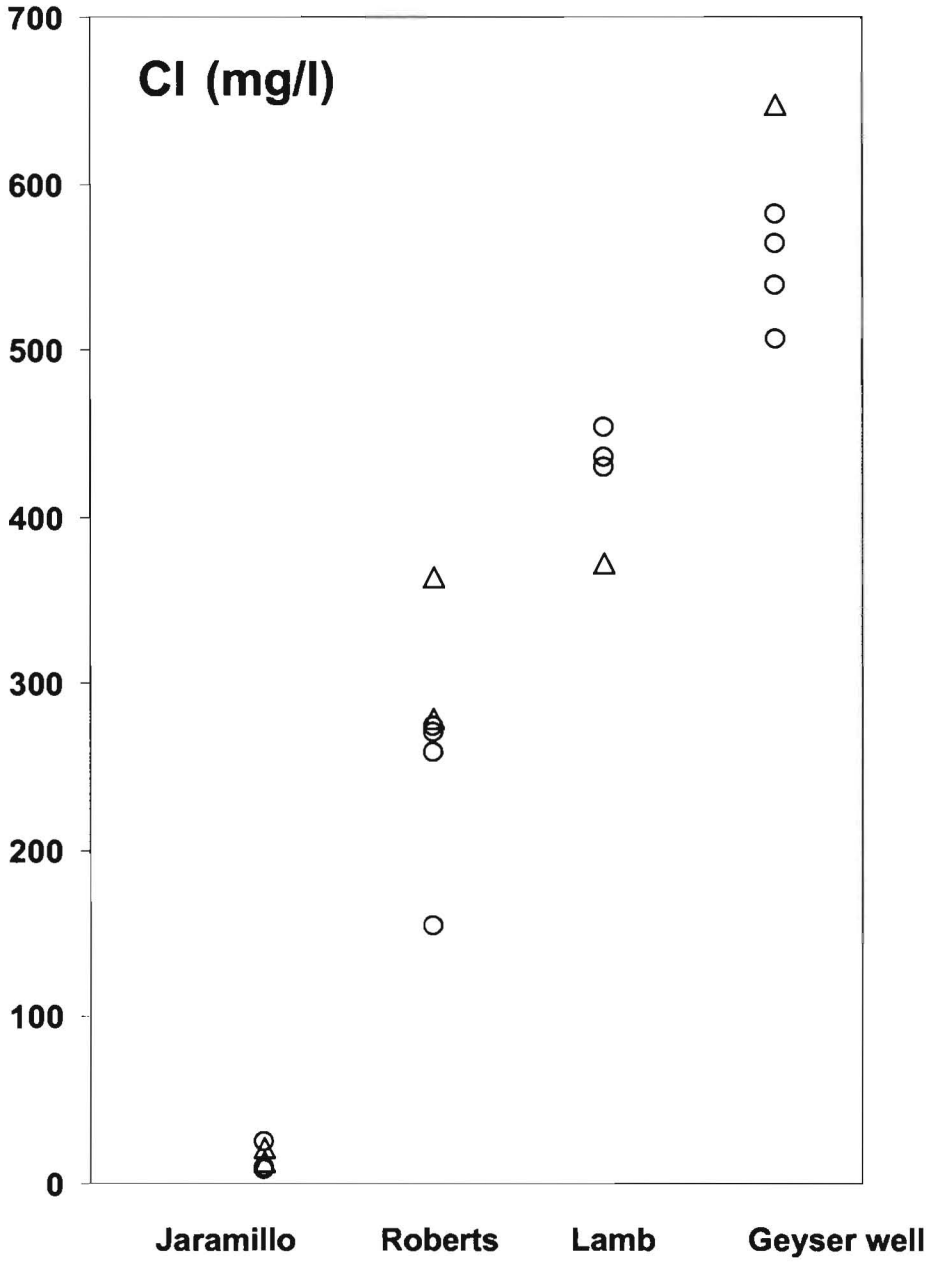

Temporal variation in four wells. Older data are taken from Cumming (1997); recent data are from this study

○ 1995-1996

△ 2008

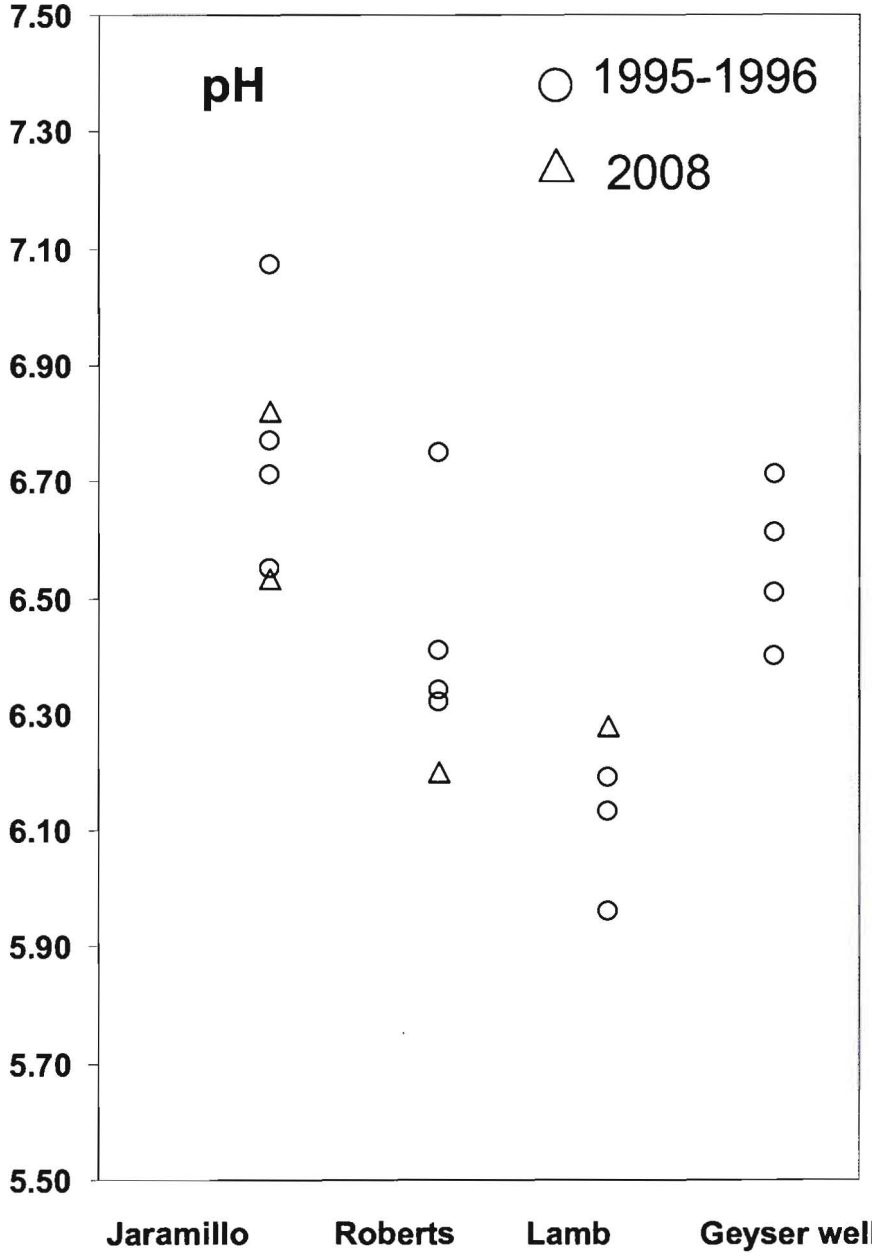
pH
1995-1996
2008
7.50
7.30
7.10
6.90
6.70
6.50
6.30
6.10
5.90
5.70
5.50
Jaramillo
Roberts
Lamb
Geyser well

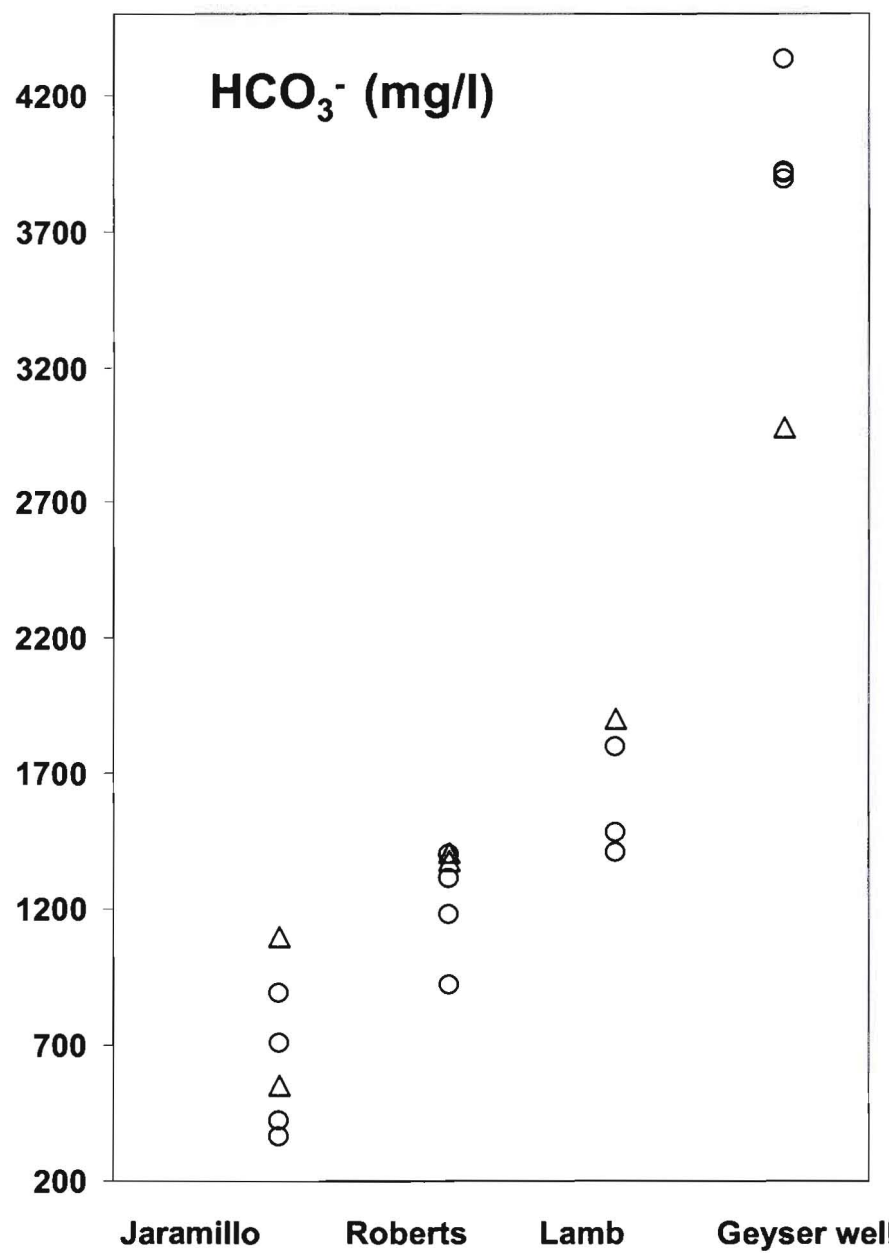
HCO3- (mg/l)
4200
3700
3200
2700
2200
1700
1200
700
200
Jaramillo
Roberts
Lamb
Geyser well